https://doi.org/10.5194/essd-2024-396
Preprint. Discussion started: 18 October 2024

Open Access Earth System Science Data Discussions

Dheed: an ERA5 based global database of dry and hot extreme events from 1950 to 2022

Mélanie Weynants[1], Chaonan Ji[2], Nora Linscheid[1], Ulrich Weber[1], Miguel D. Mahecha[2], and Fabian Gans[1]

[1]Max Planck Institute for Biogeochemistry, Jena, Germany
[2]Remote Sensing Center for Earth System Research, Leipzig University, Germany

Correspondence: Mélanie Weynants (mweynants@bgc-jena.mpg.de); Fabiam Gans (fgans@bgc-jena.mpg.de)

Abstract. The intensification of climate extremes is one of the most immediate effects of global climate change. Heatwaves and droughts have uneven impacts on ecosystems that can be exacerbated in case of compound events. To comprehensively study these events, e.g. with local high-resolution remote sensing or in-situ data, a global catalogue of such events is essential. Here, we propose a workflow to build a database of large-scale dry and hot extreme events based on data from ERA5 reanalysis. Drought indicators are constructed based on evapotranspiration and precipitation data averaged over 30, 90 and 180 days. Extreme events are detected with the peak-over-threshold approach for the 1950–2022 period. Extremes and non-extremes are defined for daily maximum temperature at 2 m in combination with three drought indicators. In the last step, the spatiotemporal extent of the events is computed by a connected component analysis. The identified events are validated against extreme events reported in the literature.

1 Introduction

Extreme weather and climate events can induce stress on ecosystems and thereby have negative impacts on society, e.g. via yield losses with unclear implications (Frank et al., 2015; Sippel et al., 2018; Mahecha et al., 2024). With Earth climate currently changing, the intensity and frequency of heat and hydroclimatic extremes are increasing (Seneviratne et al., 2023; Rodell and Li, 2023). Specifically, concerns about compound extreme weather and climate events – when multiple types of climate extremes occur simultaneously – have been raised for over a decade (IPCC, 2012). A typology to guide studies on those types of occurrences has recently been proposed (Zscheischler et al., 2020). Compound climate extremes often have more detrimental effects on vegetation growth than univariate extremes (Yang et al., 2023; Bastos et al., 2023). For instance, global increased drought and heat (DH) induced tree mortality has been highlighted in 2010 (Allen et al., 2010) and investigated ever since. Vegetation is indeed more susceptible to damage during heat extremes after exposure to drought stress, as less water is available to buffer the physiological consequences of the heat extreme (Marchin et al., 2022). The complex physiological mechanisms of increased tree mortality under a warming and drying atmosphere richer in CO_2 are, however, still debated (McDowell et al., 2022). The cascading processes triggered by concurrent DH extremes also impact society as a whole (Niggli et al., 2022), and require particular focus given the expected increasing burden on society by DH in many parts of the world.

https://doi.org/10.5194/essd-2024-396
Preprint. Discussion started: 18 October 2024

To study the impacts of dry and hot extreme events (DHEE) globally, a unified database of such events is needed. Yet, the definition of heatwaves and droughts is not standardized in the literature. The World Meteorological Organisation describes heatwaves as "periods where local excess heat accumulates over a sequence of unusually hot days and nights" (https://wmo.int/topics/heatwave), but it defines no universal indicator. The scientific literature abounds with heatwave indicators, often sector oriented (Perkins and Alexander, 2013). Many define a heatwave as a period of at least three consecutive days with maximum temperature exceeding a certain threshold (e.g., Perkins and Alexander, 2013; Russo et al., 2015; Lavaysse et al., 2018; Russo and Domeisen, 2023), either absolute or percentile based. These probabilistic thresholds can be regional or local and relative to reference periods ranging from calendar day to season or year, over spans of ten to thirty years. Droughts are prolonged dry periods that can last from weeks to years. Depending on their duration and intensity, the hydrological compartment affected differs, and so does the impact on ecosystems. One generally distinguishes between meteorological, hydrological, agricultural and socio-economic droughts (Mishra and Singh, 2010). Various indicators have been developed to characterize drought conditions. The commonly used Standard Precipitation Evaporation Index (SPEI) is a “multi-scalar drought index used to determine the onset, duration and magnitude of drought conditions" (Vicente-Serrano et al., 2010). It is generally calculated from monthly climate data, but some authors have used it with daily data to characterize drought dynamics at a finer temporal resolution (Wang et al., 2021). Indeed, Li et al. (2021) highlight the need for sub-monthly scale indices to monitor short term compound dry and hot conditions. The rationale is that, otherwise, e.g. a four week drought happening across two months might remain undetected in monthly data. A recent study proposes to calculate the daily SPEI using nonparametric Kernel Density Estimation (KDE) and then transform the KDE based quantiles into standardized normal scores, thereby avoiding fitting a parametric distribution to the data (Pohl et al., 2023). As sub-monthly dry and hot conditions – or even a few hot days – can propagate into impacts, and heatwaves and droughts evolve on different time scales, we find it advantageous to work on data with daily resolution, and with multi-scalar drought indicators representing water budgets for different temporal windows.

Studies have often focused on single compound events (Flach et al., 2018; Ciais et al., 2005; Bastos et al., 2020, e.g.,), on specific regions or measurement stations (Li et al., 2021; Pohl et al., 2023, e.g.,), but to the best of our knowledge no global gridded analysis of DHEE at daily scale has been published so far. Therefore, here we propose Dheed, a database of large-scale dry and hot extreme events derived from the analysis of long time series of the ERA5 global climate reanalysis provided by the European Centre for Medium Range Weather Forecasts (ECMWF) (Hersbach et al., 2020, 2023). Dheed provides the potential for analyzing historical patterns and trends in heatwaves and droughts over time and facilitates detailed studies on the impact of dry and hot climate extremes on ecosystems, species, and regions. For example, it can serve for driving the sampling of minicubes of high-resolution satellite imagery – e.g., Copernicus Sentinel-2 data (Ji et al., 2024) – to train models predicting ecosystem states (Requena-Mesa et al., 2021; Benson et al., 2023) under extreme climate conditions. Dheed can also be used to assess the capacity of ecological monitoring networks to detect impacts of dry and hot extreme events (Mahecha et al., 2017). Further potential applications encompass site selection for studying the effects of extreme dry and hot conditions on specific species or targeted sampling of high-resolution Earth Observation data for impact research, e.g. assess and forecast carbon sequestration loss during extremes, or cropland productivity loss. Hereafter, we describe the data and methods employed to

https://doi.org/10.5194/essd-2024-396
Preprint. Discussion started: 18 October 2024

build Dheed, we present a brief global and continental analysis of trends in DHEE and we benchmark detected DHEE against events reported in the literature.

2 Data and methods

Our approach draws on the concept of analysis-ready data cube, particularly useful in Earth system science to access and analyse multiple data dimensions, such as variable, spatial and temporal (Mahecha et al., 2020). The first step in building Dheed consists of a temporal analysis of climate reanalysis data to detect extreme values in time series of temperature and drought indices, which we further refer to as Discrete Extreme Occurrences (DEOs). It is followed by a spatio-temporal connected component analysis to group DEOs connected in space and time into uniquely labelled Dry and Hot Extreme Events (DHEEs) (Zscheischler et al., 2013; Lloyd-Hughes, 2012) that can then be compared to events reported in the literature. The workflow, detailed below and illustrated in Figure 1, runs entirely in Julia, relying largely on the YAXArrays.jl package (Gans et al., 2023). All figures are created with Makie.jl (Danisch and Krumbiegel, 2021).

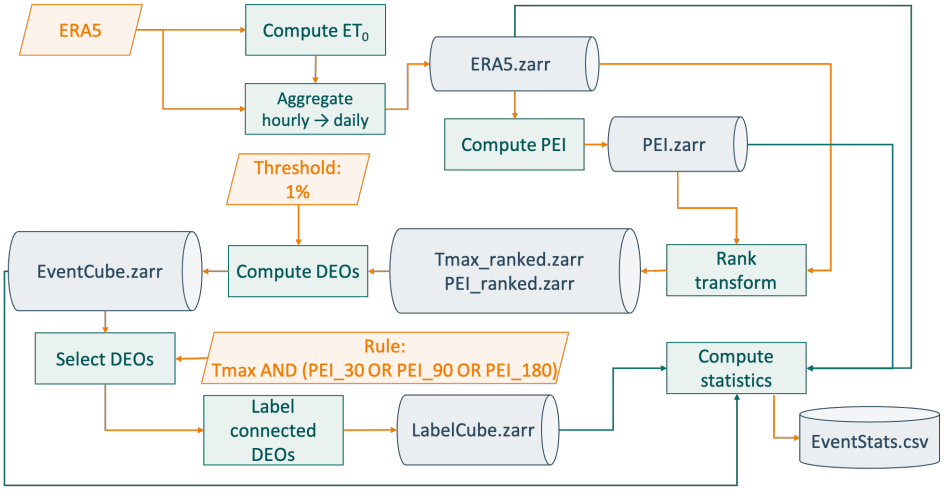

Figure 1. Workflow for the detection of dry and hot extreme events. ET_{ref} is the reference evapotranspiration, PEI is a Precipitation–Evapotranspiration based indicator, Tmax is the daily maximum temperature at 2 m. DEOs are Discrete Extreme Occurrences, i.e. extreme values in the time series of temperature and drought indices. Dheed, the resulting dry and hot extreme events database consists of the EventCube, the LabelCube and the EventStats table.

2.1 Climate data pre-processing

The workflow exploits the hourly gridded ERA5 data, from 1950 to 2022 (Hersbach et al., 2023). Specifically, the following variables are used: temperature at 2 meters (T_{2m}) [K], 10 meter wind speed: zonal ($u10$) and meridional ($v10$) components [ms^{-1}], atmospheric surface pressure (sp) [Pa], surface net solar and thermal radiation (ssr and str) [Jm^{-2}], saturation

https://doi.org/10.5194/essd-2024-396
Preprint. Discussion started: 18 October 2024

water vapour pressure ($swvp$) [hPa], vapour pressure (vp) [hPa] and total precipitation (tp) [m]. Grid cells from the ERA5 land mask with a value greater than 0.5 are considered land. Data are aggregated over time from hourly to daily time steps, by calculating the daily mean, minimum, and maximum for T_{2m}, and the cumulative values for tp and ET_{ref} (see hereafter). When aggregating to daily time steps, a day includes all time steps from 0:00 to 23:00 UTC for all grid cells. Hence, aggregation windows do not correspond to local calendar days. The resulting data are stored in a data cube in Zarr format with the following chunk sizes: longitude = 60, latitude = 60, time = 5,844, suited for time series analysis. As in the original ERA5 data, the longitude axis ranges from 0 to 360 degrees. The spatial resolution is 0.25 degree in both latitude and longitude, i.e., the longitude and latitude dimensions are 1,440 and 721 respectively. After aggregation of the hourly data to daily temporal resolution, each time series has 26,663 data points over the period going from 1 January 1950 to 31 December 2022.

The hourly reference evapotranspiration for a well watered grass cover (ET_{ref}) [mm hr^{-1}] is calculated with the FAO's Penman-Monteith equation (Allen et al., 1998) from the above mentioned ERA5 variables, following appropriate units adjustments and assumptions (Singer et al., 2021):

$$\mathrm{ET}_{ref} = \frac{0.408\Delta(R_n - G) + \gamma \frac{37}{\theta_{2m}+273} u_2 (swvp - vp) \times 10^{-1}}{\Delta + \gamma(1 + C_d u_2)} \tag{1}$$

where R_n is the surface net radiation [$\mathrm{MJm}^{-2}\mathrm{hr}^{-1}$]), calculated as $(ssr + str) \times 10^{-6}$, G is the soil heat flux density at the soil surface [$\mathrm{MJm}^{-2}\,\mathrm{hr}^{-1}$] conditioned on the time step, with values differing between daytime and nighttime ($G = R_n \times 0.1$ if $R_n < 0.0$, $G = R_n \times 0.5$ otherwise) and set to 0 where water covers more than 50% of the spatial grid cell, $\theta = T_{2m} - 273.15$ is the mean daily air temperature at 2 m height [°C], u_2 is the wind speed at 2 m height [$\mathrm{m\,s}^{-1}$], calculated from u_{10} and v_{10} using the log wind profile (Equation 2), Δ is the slope of the vapour pressure curve [$\mathrm{kPa°C}^{-1}$], γ is the psychrometric constant [$\mathrm{kPa°C}^{-1}$] and C_d is a time step dependent coefficient. Δ and γ are calculated from sp and θ_{2m} according to FAO recommendations (Allen et al., 1998) with equations 3 and 4.

$$u_2 = \sqrt{u_{10}^2 + v_{10}^2} \frac{4.87}{\log(67.8 \times 10 - 5.42)} \tag{2}$$

$$\Delta = 4098.0 \frac{0.6108 \exp \frac{17.27\theta_{2m}}{\theta_{2m}+237.3}}{(\theta_{2m} + 237.3)^2} \tag{3}$$

$$\gamma = cp \frac{sp}{\epsilon\lambda} \tag{4}$$

where $\lambda = 2.45$ is the latent heat of vaporization [MJ kg -1] (simplification in the FAO PenMon (latent heat of about 20°C), $cp = 1.013 \times 10^{-3}$ is the specific heat at constant pressure [MJ kg-1 °C-1] and $\epsilon = 0.622$ is the ratio between molecular weight of water vapour and dry air. According to Walter et al. (2001), C_d should vary between daytime (0.24) and nighttime (0.96), but adopting the constant value for daily calculation (0.34) has a negligible effect when values are aggregated by day ($< 10^{-6}$).

https://doi.org/10.5194/essd-2024-396
Preprint. Discussion started: 18 October 2024

Open Access Earth System Science Data Discussions

For the purposes of this dataset, daily drought conditions need to be assessed to be later analyzed together with a daily heatwave indicator to detect extreme events at daily resolution (Li et al., 2021). Therefore, the daily average water balance $\text{PEI}_{N,i}$ for day i in the time series over the N antecedent days is calculated as an indicator of drought, accounting for different hydrological compartments of ecosystems:

$$\text{PEI}_{N,i} = \frac{1}{N} \sum_{j=i-N-1}^{i} (tp_j \times 10^{-3} - \text{ET}_{ref,j}) \tag{5}$$

with $N \in (30, 90, 180)$ to obtain PEI_{30}, PEI_{90}, and PEI_{180}. Following the convention used in ERA5, downward fluxes have positive values. Extreme dry values are hence those for which PEI_N is small.

2.2 Event detection

The detection of DEOs is based on a purely probabilistic threshold applied to the empirical distribution of the indicators. In each spatial grid cell, we examine the temporal distribution of each of the four indicators independently (T_{max}, PEI_{30}, PEI_{90}, and PEI_{180}). Fitting a parametric distribution to the time series of the drought indicators to obtain a standarized index (SPEI) proved difficult for many grid cells. Instead, the values were rank-transformed to obtain their empirical distribution function, as an estimate of the cumulative distribution function of each spatial grid cell. We applied the same rank-transformation to T_{max} values after reversing them so that the extremes of interest are consistently the smallest values for all four indicators. We choose an absolute threshold specific to each grid cell to focus on extreme hot conditions, and do not consider here winter heatwaves. We set the lowest 1% of the empirical cumulative distribution as extreme. We synthesize the DEOs of the four indicators in a single variable encoded as an 8-bit integer by assigning a specific bit to each indicator. DEOs of T_{max} activate the first (smallest) bit, PEI_{30} the second, PEI_{90} the third, and PEI_{180} the fourth. The fifth bit encodes for all values that lie outside the tails of all four distributions, i.e., that have values between 0.1 and 0.9. These values are stored in a data cube named `EventCube` (Fig. 1).

From the EventCube, we extract DHEEs as labelled groups of connected dry and hot DEOs (Zscheischler et al., 2013; Lloyd-Hughes, 2012). We restrict the analysis to spatio-temporal grid cells of the EventCube that have uneven values greater than 1, i.e. DEOs that are flagged as both hot and dry extremes. Moreover, using *ImageFiltering.jl* (Ima, 2023a), we filter for events that last at least three consecutive days. The connected component labelling algorithm assigns a unique label to each group of connected DEOs, looking for six way connections. Each grid cell with coordinates $(x \pm 1, y, z)$, $(x, y \pm 1, z)$ or $(x, y, z \pm 1)$ is connected to the grid cell at (x, y, z) , with x, y and z the longitude, latitude and time, respectively. We modify the *ImageMorphology.label_components* function (Ima, 2023b) to group DEOs connecting across the globe along the longitude dimension. We also introduce the possibility to merge labels from contiguous data cubes. We store the resulting labelled dry and hot extreme events in a data cube named labelCube. Figure 2 illustrates the entire workflow with the example of the 2003 summer heatwave in Europe (Event 33 in Table A1.

For each labelled DHEE, we compute the following properties:

https://doi.org/10.5194/essd-2024-396
Preprint. Discussion started: 18 October 2024

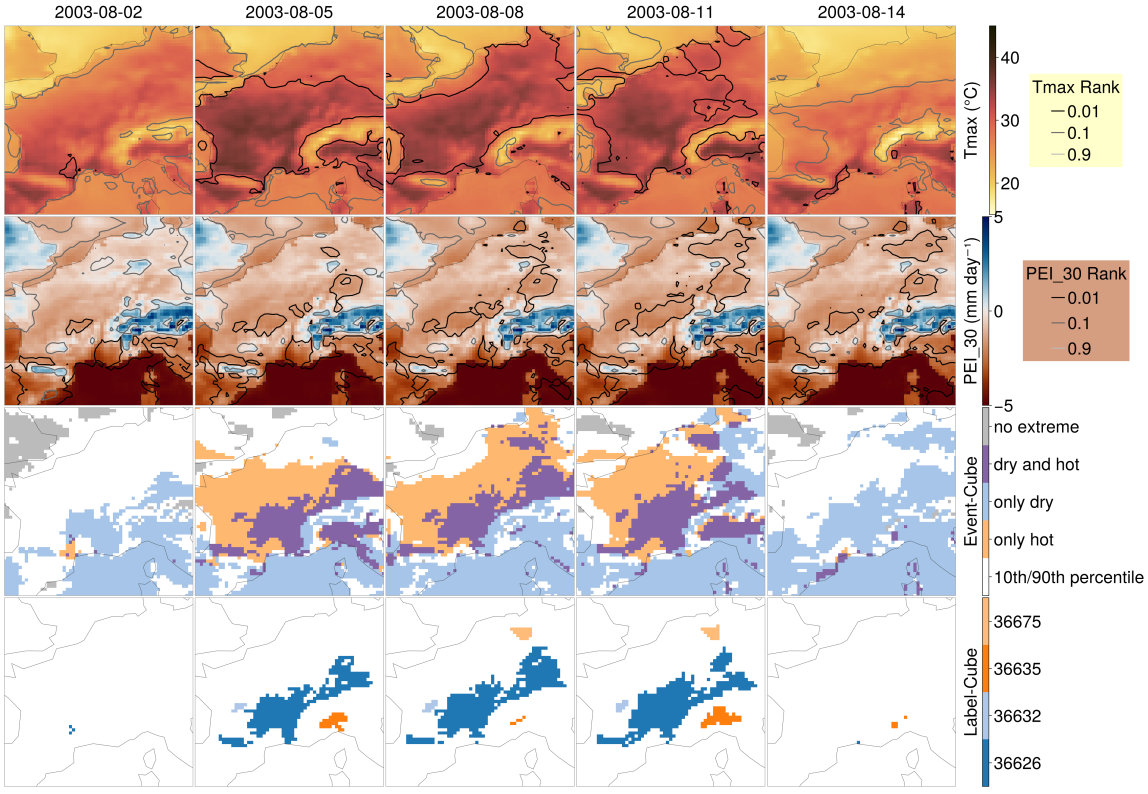

Figure 2. Example of dry and hot extreme event detection workflow over the 2003 summer heatwave in Europe. Columns show the time evolution of the data sampled at every 4th time step from Aug 1 to Aug 13 2003. Row 1 and 2 show the raw daily maximum 2m air temperature with isolines for the grid cell based 1%, 10% and 90% threshold. The third row shows the encoding into the EventCube where single voxels can be marked as only extremely dry, only extremely hot, a combination of both or none of them, while voxels plotted as white are in a regime of normal conditions between 0.1 and 0.9 percentile. Through a connected component analysis in space and time these voxels are connected into four connected components that are registered as separate labelled events in the Dheed dry and hot extreme events database.

- spatio-temporal bounding box (`start_time`, `end_time`, `longitude_min`, `longitude_max`, `latitude_min`, `latitude_max`),
- statistics on the the indicators (`t2mmax_mean`, `t2mmax_min`, `t2mmax_max`, `pei_30_mean`, `pei_30_min`, `pei_30_max`, `pei_90_mean`, `pei_90_min`, `pei_90_max`, `pei_180_mean`, `pei_180_min`, `pei_180_max`),
- percentage of the event affected by a single indicator (`heat`, `drought30`, `drought90`, `drought180`, `compound`),
- percentage of the event that occurred over land (`land_share`),
- a proxy of the total volume of the event as the number of voxels weighted by cos(latitude) (`volume`),

https://doi.org/10.5194/essd-2024-396
Preprint. Discussion started: 18 October 2024

- the event duration as `end_time` − `start_time` + 1day (`duration`),
- a proxy of the event total affected area as the ratio between `volume` and `duration` (`area`).

These statistics are stored in a csv table named EventStats (Fig. 1) and constitute the core of Dheed, along with EventCube and labelCube. In the next section, we present a brief analysis of these labelled DHEEs and track the ten largest in `volume` and the ten longest in `duration` in the scientific literature. To assess the reliability of the event detection method, we also compare a set of historical events reported in the scientific literature or the media with the Dheed. All labelled events that intersect with the spatio-temporal window reported in Table A1 are selected from the labelCube. Their statistics are extracted from the EventStats and evaluated.

3 Results

3.1 Indicators of dry and hot conditions

All detected daily time points of extreme heat or drought (DEOs) from 1950-2022 are recorded in the EventCube. This data cube can be used to analyse time series of DEOs at specific locations. For example, Figure 10 shows the event type along with $T_{2,max}$ from the ERA5 daily data cube and the PEIs for a few days in the summer of 2021 at Lytton, British Columbia, Canada. Longer time series can also be easily analysed (Figures A1 and A2). Beyond analysing single locations, the dataset allows to draw a general overview of the regional or global trends in dry and hot extremes. Figure 3 shows DEOs globally aggregated by year and by type of extreme, over land only, from 1970 to 2022. The percentage is the sum of land grid cells weighted by the cosine of their latitude, representing the annual number of days × area, reported on the total number of land grid cells multiplied by the cosine of their latitude in that year, representing the total land area multiplied by the number of days in the year. The further back in time, the larger the uncertainties in the reanalysis data, due to a lack of observations to be assimilated with the numerical model results, especially in the southern hemisphere. No satellite data were used in ERA5 before 1970 (Hersbach, 2023), leading to yet larger uncertainties in the southern hemisphere. Therefore, we do not include the years 1950–1969 in the analysis. Figure 3 shows DEOs by event type aggregated globally over land by year. The compound dry and hot DEOs shown in purple represent only a small fraction of the extreme dry or hot conditions. The inter-annual variability is large, but there seems to be a positive trend. Figure 4 shows the DEOs aggregated by macro type of extreme, which means the bars may not be cumulated. By our definition of the extremes, since we applied a 1% threshold on the time series, the relative annual number of days and area affected by these extremes expressed in percentage for each macro type is 1% on average over the complete time series (1950–2022). Values vary however from year to year. A Theil-Sen approximation of the trend over time shows that all three drought indicators have a positive trend. Surprisingly the trend for maximum temperature extremes is not significant (p–value of Mann–Kendall test greater than 0.05). This suggests that the extents of short term (d30), midterm (d90) and longer term (d180) droughts are increasing at a similar pace. Figure 5 shows only grid cells affected by compound dry and hot extremes aggregated globally by year. The values are an order of magnitude smaller than with the univariate extremes, but the trend is such that there was a tripling of the annual affected area over the 53 years investigated. Figure 6 and Table 1 show

https://doi.org/10.5194/essd-2024-396
Preprint. Discussion started: 18 October 2024

Open Access Earth System Science Data Discussions

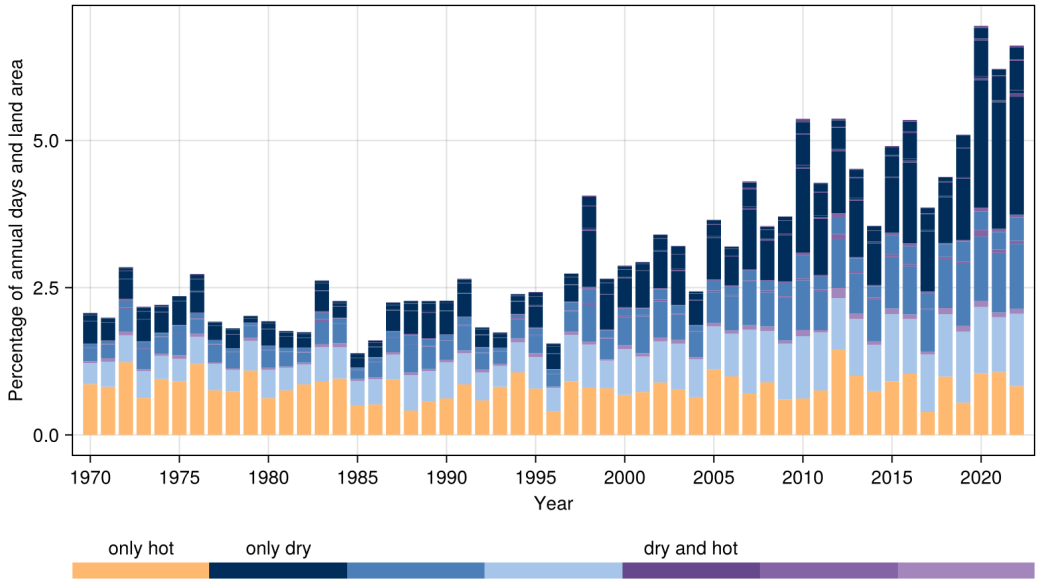

Figure 3. Annual spatiotemporal extent of extreme dry and hot days, by the value of data in EventCube. The sum of Discrete Extreme Occurrences (DEO) of a given value weighted by the cosine of the grid cell latitude is divided by the sum of all land voxels in a given year, expressed as percentage.

a continental aggregation of the annual `volume` affected by compound dry and hot DEOs. The trends and average values are not uniform across continents. With 0.03 %, Antarctica is the least affected continent, well below the global average of 0.13 %. Australia and South America are below average with 0.10 and 0.11 %. However, they saw a steep increase of extreme dry and hot days in recent years, reaching averages close to or above the global average for the period 2000-2022. Europe is the continent most affected by compound dry and hot events, followed by Africa. Africa is the continent that has experienced the steepest increase in annual cumulative area subject to compound extreme dry and hot days.

3.2 Database of dry and hot extreme events

Extreme events in which heat and drought coincided were labelled and characterized further. The labelled extreme events include only DEOs where dry and hot extreme conditions were observed for at least three consecutive days. Although the connected components algorithm was run over all grid cells, the statistics for the labelled events were computed over land only. In total, the database contains 26,351 unique labelled events for the years 1970 to 2022. Most events have a `duration` of four days and a spatial extent smaller than a grid cell at the equator (`area`) (Fig. 7, left). In recent years, there were more dry and hot extreme events (Fig. 7, right). The distribution of their `volume` remains however stable over time. Nevertheless, seven of the ten largest events occurred after the year 2000. They are listed in Table 2 (top) along with the ten longest events (bottom).

https://doi.org/10.5194/essd-2024-396
Preprint. Discussion started: 18 October 2024

Open Access Earth System Science Data Discussions

Table 1. Average percentage of annual extremely dry and hot days and area by continent and globally, over the total analysis period (1970-2022), over the first 30 years (1970-1999) and over the recent years (2000-2022).

Continent	Years_1970_2022	Years_1970_1999	Years_2000_2022
Africa	0.15	0.06	0.26
Asia	0.14	0.11	0.17
Australia	0.10	0.04	0.17
North America	0.14	0.11	0.19
Oceania	0.13	0.10	0.18
South America	0.11	0.05	0.20
Antarctica	0.03	0.02	0.04
Europe	0.21	0.13	0.31
Global	0.13	0.08	0.19

Table 2. Biggest labelled dry and hot extreme events in the period 1970–2022: Ten largest in `volume` and ten longest in `duration`.

		Date		Longitude		Latitude				
rank	label	start	end	min	max	min	max	`duration`	`area`	`volume`
1	42561	2010-07-12	2010-08-21	28.00	63.25	36.25	64.25	41 days	1640.94	67278.7
2	51252	2016-10-07	2016-11-04	13.50	34.50	-24.00	-5.75	29 days	1266.11	36717.1
3	24092	1983-03-01	1983-03-30	0.00	359.75	1.75	10.25	30 days	685.372	20561.2
4	55983	2021-02-20	2021-03-16	16.50	31.25	-2.50	10.00	25 days	698.638	17465.9
5	55755	2020-09-30	2020-10-14	288.25	316.75	-23.25	-10.75	15 days	980.048	14700.7
6	25632	1986-07-02	1986-07-22	102.00	135.25	54.75	65.25	21 days	609.035	12789.7
7	18958	1972-08-18	1972-08-30	31.00	51.50	47.75	60.75	13 days	763.996	9931.95
8	44770	2012-06-17	2012-07-04	247.75	259.50	26.75	41.75	18 days	485.379	8736.83
9	36790	2003-10-03	2003-10-19	18.50	31.25	-21.50	-6.25	17 days	486.031	8262.52
10	53015	2019-01-11	2019-01-26	123.25	149.00	-36.0	-23.75	16 days	510.833	8173.33
1	31767	1998-03-01	1998-04-27	115.00	118.50	-1.25	3.25	58 days	67.1294	3893.51
2	31866	1998-03-07	1998-04-30	115.00	118.50	4.00	6.50	55 days	20.7583	1141.71
3	49981	2015-09-13	2015-10-26	123.00	124.75	0.50	1.25	44 days	7.43092	326.96
4	44843	2012-06-23	2012-08-04	229.25	272.25	69.75	78.50	43 days	47.4123	2038.73
5	18998	1972-09-10	1972-10-21	109.25	116.25	-3.75	-0.25	42 days	85.2228	3579.36
6	24109	1983-03-01	1983-04-11	114.50	118.50	-2.00	4.25	42 days	58.1754	2443.37
7	42561	2010-07-12	2010-08-21	28.00	63.25	36.25	64.25	41 days	1640.94	67278.7
8	28223	1992-03-25	1992-04-30	98.50	105.00	12.75	20.25	37 days	135.121	4999.47
9	50340	2016-02-27	2016-04-02	283.50	288.00	6.75	11.00	36 days	57.2994	2062.78
10	54071	2020-03-06	2020-04-09	80.00	80.75	6.00	7.50	35 days	8.14539	285.089

https://doi.org/10.5194/essd-2024-396
Preprint. Discussion started: 18 October 2024

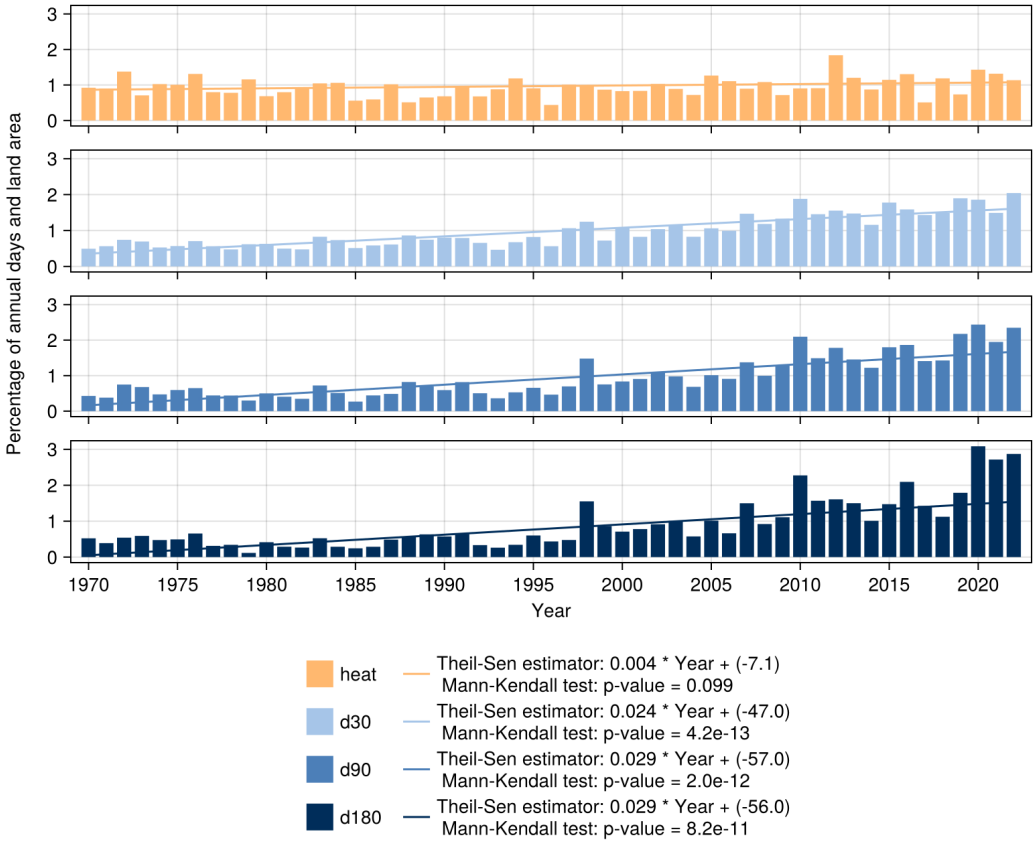

Figure 4. Annual spatiotemporal extent of extreme dry and hot days, by type of extreme. The sum of Discrete Extreme Occurrences (DEO) combined by type of event and weighted by the cosine of the grid cell latitude is divided by the sum of all land voxels in a given year, expressed as percentage.

Figure 8 shows the ten largest labelled events that occurred in the years 1970 to 2022. The largest event overall – labelled 42561 – relates to the Russian heatwave of 2010 (e.g. Flach et al., 2018). It also appears as the seventh longest dry and hot event globally over the same period (Table 2, bottom). Events labelled 51252 (second largest) and 36790 (ninth largest) can be linked to the El Niño induced droughts in southern Africa in 2002–2003 and 2015–2016 Rouault et al. (2024). Event labelled 24092 in Western and central Africa in 1972 can be traced back to the extreme drought of 1972–1973 (Masih et al., 2014). The serious drought of 2021 in Central Africa, which compounded the humanitarian situation caused by COVID-19, internal conflicts, and plague locusts in the region (Hassan et al., 2023), is captured in Event 55983. A severe drought-complex hit over the Pantanal and other regions in South America in October 2020, increasing fires and impacts on natural and human systems (Marengo et al., 2022), to which Event 55755 can be associated. In the spring and summer of 2012, the United States of America suffered through their hottest year on record, which complicated and exacerbated the ongoing drought situation

https://doi.org/10.5194/essd-2024-396
Preprint. Discussion started: 18 October 2024

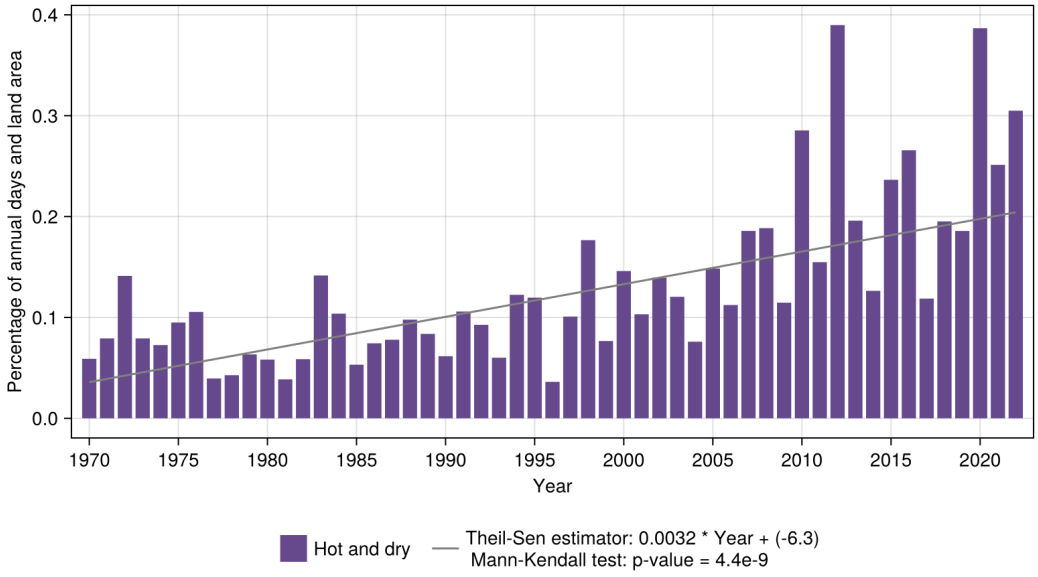

Figure 5. Annual spatiotemporal extent of extreme compound dry and hot days. The sum of Discrete Extreme Occurrences (DEO) that are both dry and hot weighted by the cosine of the grid cell latitude is divided by the sum of all land voxels in a given year, expressed as percentage.

(Rippey, 2015). Event 53015 occurred in January 2003, which was Australia's hottest during the country's hottest summer on record (http://www.bom.gov.au/climate/current/month/aus/archive/201901.summary.shtml, Accessed 12 August 2024). No references could be found to Events 25632 and 18958, which occurred in Siberia in July 1986 and Russia in 1972, respectively.

El Niño–induced droughts in Malaysia/Indonesia (Borneo-Kalimantan Island) in 1972-1973, 1982-1983, 1997-1998, 2014-2016 are captured in the longest events 18998, 24109, 31767, 31866, 49981 (Table 2, bottom), which contributed to triggering increased forest mortality (Allen et al., 2010). The long event 44843 in the Canadian-Arctic Archipelago in the summer of 2012 can be linked to the summer heatwave that affected North America. A mega-drought was reported in Colombia in 2015-2016, which was accompanied by a strong warming in the Amazon forest (Weng et al., 2020) and can be linked to the long event 50340 that occurred in February-April 2016. No specific references were found to the long events 28223 in Mainland Southeast Asia (Indochina Peninsula) in 1992 and 54071 in Sri Lanka in March 2020.

3.3 Validation

Next to the largest and longest extreme dry and hot events discussed in the previous section, the database was tested against a list of extreme events gathered independently and a priori (Table A1). The intersection of the reported approximate footprint and time range of those events with the database proposed here is summarized in Figure 9. Reported events are generally associated with a few large labelled events and with many small labelled events. This is consistent with the distribution of the

https://doi.org/10.5194/essd-2024-396
Preprint. Discussion started: 18 October 2024

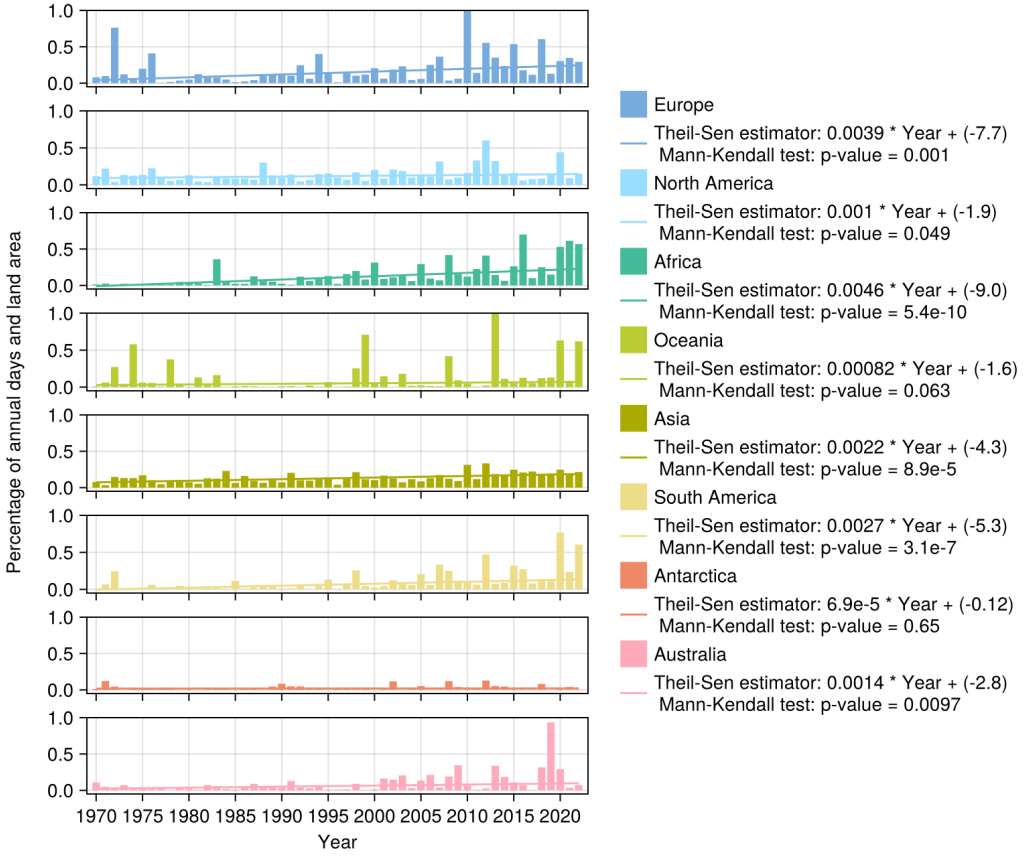

Figure 6. Annual spatiotemporal extent of extreme dry and hot days, by continent. The sum of both dry and hot Discrete Extreme Occurrences (DEO) weighted by the cosine of the grid cell latitude is divided by the sum of all land voxels in a given continent and year, expressed as percentage. The y axis is limited to 1.0 %, but the bar for the year 2010 in Europe extents to 1.8 % and that of the year 2013 in Oceania to 1.1 %.

size of the labelled events (Figure 7). However, some reported events (8, 25, 28, 31, 36, 39) intersect with none in the database. These are either reported heatwaves or droughts, and one reported compound event. Focusing on one grid cell of that particular reported compound event in Canada (obs_event 8 in Table A1), Figure 10 shows that, although both dry and hot conditions were observed over its reported course, they did not coincide according to the stringent threshold used in this study. When the strong heatwave started on 25 June 2021, the PEI values were still above the 10th percentile. Later, they dropped under the first percentile, but the maximum daily temperatures, although above the 90th percentile, remained below the 99th percentile except for two consecutive days, without reaching the three consecutive days necessary to qualify as an extremely dry and hot event in the database proposed here. The summer heatwave of 2022 in Tunisia (event 25) did not trigger the detection workflow presented here (Suppl. Fig A3). Although the PEI_{30} did drop below the 1st percentile, the ERA5 maximum temperature did

https://doi.org/10.5194/essd-2024-396
Preprint. Discussion started: 18 October 2024

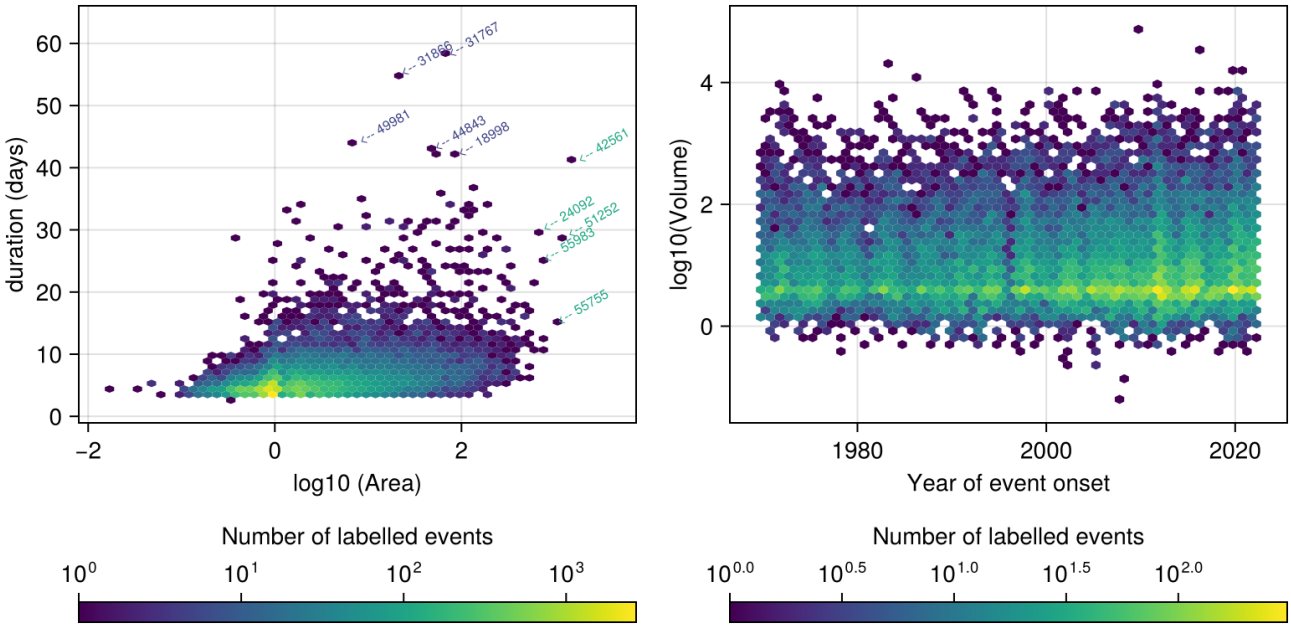

Figure 7. Two-dimensional histograms of labelled events over land only in the years 1970 to 2022. Left: Duration versus area of events. Labels indicate the five events with the largest volume (green) and the longest duration (blue); Right Volume of event versus year of event's onset.

not reach the 48 ° C reported in Tunis on 13 July 2022 (Pratt, 2022) and the indicator stayed under the 99th percentile. The Southern Great Plains drought of 2006 (event 31) occurred in winter and was hence not associated with a heatwave as defined in this study. The 1993 drought in North East Brazil (event 36) and the Sahel drought (event 39) of 1983-1984 were not associated with heatwaves, although extreme heat and drought coincided in the previous hydrological year in the Sahel (reported event 40).

4 Discussion and outlook

The global event detection of compound dry and hot extreme events faces the difficulty of dealing with processes that happen at different time scales. Droughts occur over months and years while heatwaves take place over a few days or weeks. Computing a global standardized drought index based on daily data proved difficult. Instead, we rely on the empirical probability distribution of the drought and heat indicators. The local rank-transformation assumes that the number of extremes is the same in each grid cell, defined by a global probability. Finding a good threshold for defining extreme events on daily data was also challenging. Selecting DEOs that are too frequent leads to connectivity issues and very large labelled events spanning over the whole globe. Part of the problem was that the connected component analysis for the event detection is run on an equi-rectangular

https://doi.org/10.5194/essd-2024-396
Preprint. Discussion started: 18 October 2024

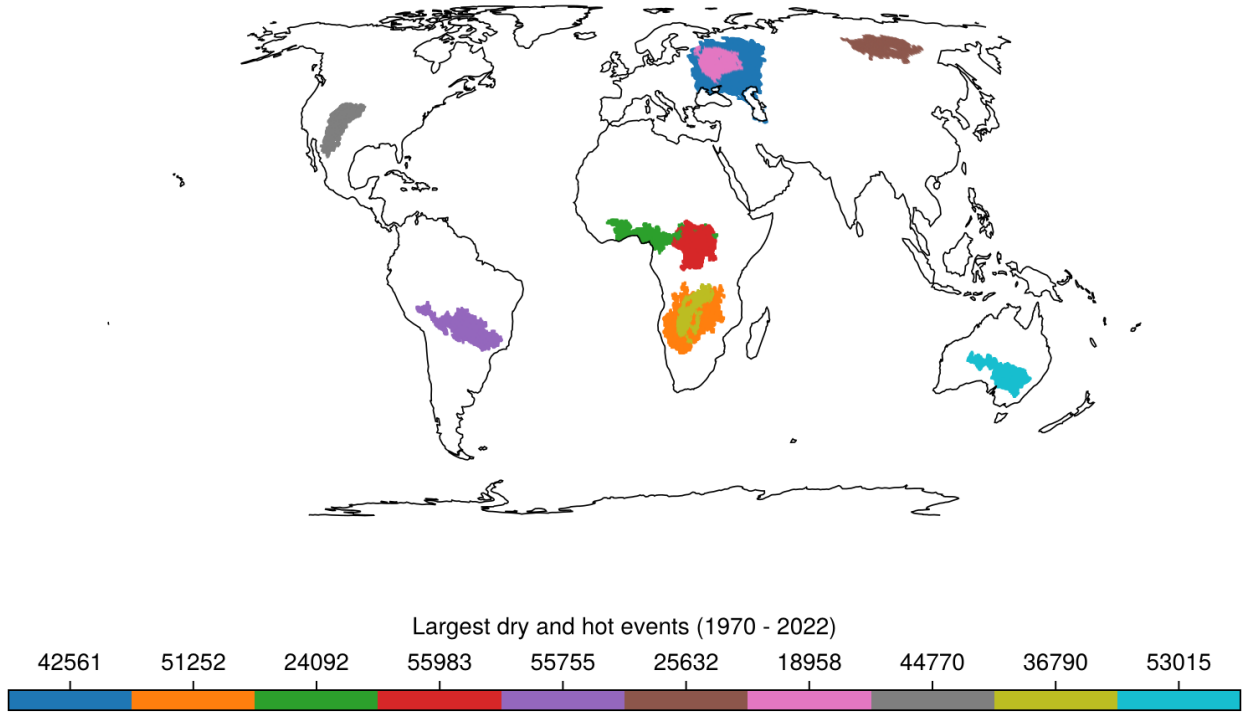

Figure 8. Spatial footprint of the ten largest labelled dry and hot events detected in this study from 1970 to 2022 over land.

grid, which leads to a bias towards more connections and larger events in high latitudes. We tested different thresholds and spatial filtering of extreme event scores respecting the spherical nature of the Earth to find a balance between the detection of documented events and avoiding too large events. Other authors have reported similar difficulties when tuning a clustering algorithm to build a database of drought events (Cammalleri et al., 2023). The final threshold is a compromise between the `volume`, `duration` and spatial footprint of the largest labelled extreme events and the effective detection of reported extreme events. We prefer smaller events to very large ones, even if a reported event is then associated with multiple smaller labelled events from our database. The framework presented here concentrates on detecting and labelling droughts and heatwaves and their compound occurrence based on daily meteorological data. The resulting labelled events can be used to analyze trends at regional, continental and global scales and to drive further research into the impacts of such events on ecosystems, specific species or society. For example, it has been firstly used as a basis for sampling high-resolution satellite imagery (Ji et al., 2024) to investigate how these compound dry and hot extreme events impact the performance of models predicting the ecosystem state. In addition, the combination of the atmospheric extreme event database and the satellite imagery describing the ecosystem

https://doi.org/10.5194/essd-2024-396
Preprint. Discussion started: 18 October 2024

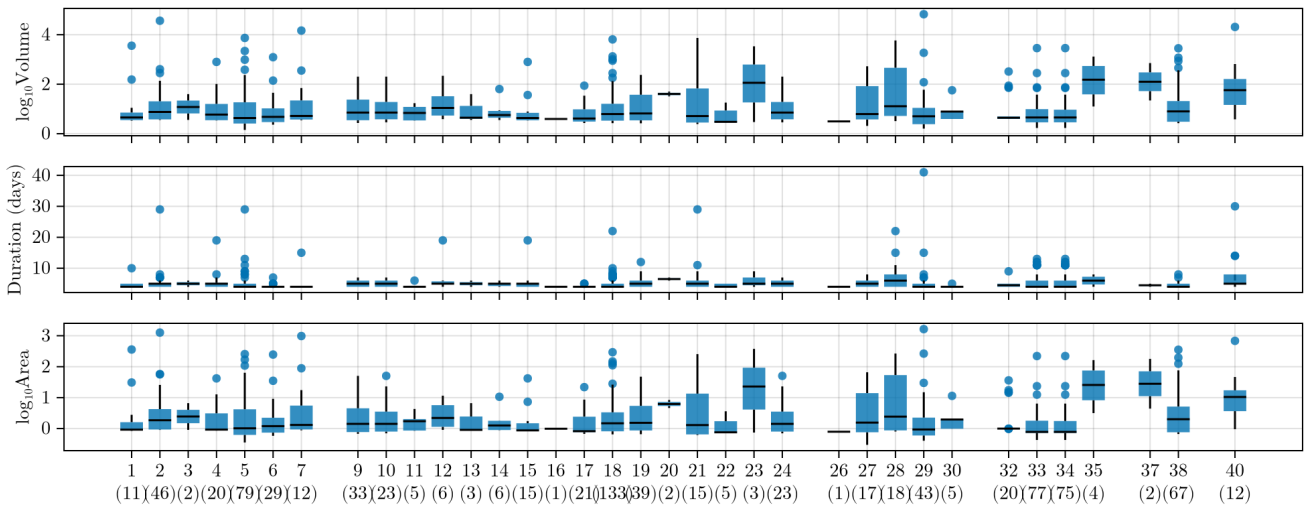

Figure 9. Validation of database. `Volume`, `Duration`, `Area` and number (between brackets) of labelled events intersecting the spatio-temporal footprint of events reported in Table A1. An empty space is left for reported events with no intersecting labelled events.

responses can help to improve our understanding of the conditions under which a certain atmospheric extreme event will have impacts on the biosphere.

In the present case, the database includes only dry and hot compound events. However, the event detection pipeline is set up to be used in a generic way and could produce event databases for different sorts of events. For example, it would be interesting to investigate other types of meteorological extreme events, e.g. involving heavy precipitation, storms, extreme cold and their combinations with heatwaves and droughts. These databases could then be used on their own or for determining areas of interest where they can be combined with other data streams, e.g. to study time series of high-resolution satellite imagery. In addition to the potential of investigating other event types, methodological improvements to the event detection pipeline are envisioned in future research. The connectivity problem at high latitudes can be addressed using other spatial filtering of extreme event scores respecting the spherical nature of the Earth, or even running the detection pipeline on grid systems with less distortion (DGGS). Besides, the current workflow is based on univariate distributions of indicators of extreme conditions. The compound nature of multi-hazard extreme events could be better apprehended with multivariate distributions. For example, standard multivariate normal kernel has been shown to outperform univariate extreme event detection on synthetic data (Flach et al., 2017) and successfully applied on real Earth system data to detect anomalies (Flach et al., 2021). Moreover, the addition of new data to the database currently necessitates to run again the complete workflow to update the rank transformed indicators. It also bears the risk that previously detected extremes don't appear as extremes if there is a distribution shift, which seems to be the case as shown in Figure 5. Besides, the labels would not be consistent across versions. Hence, in future versions, we will determine the thresholds based on a reference period, which will facilitate the addition of updated data and will ensure that previously detected extreme events stay valid. In its current state, the database records the extreme events, but not their

https://doi.org/10.5194/essd-2024-396
Preprint. Discussion started: 18 October 2024

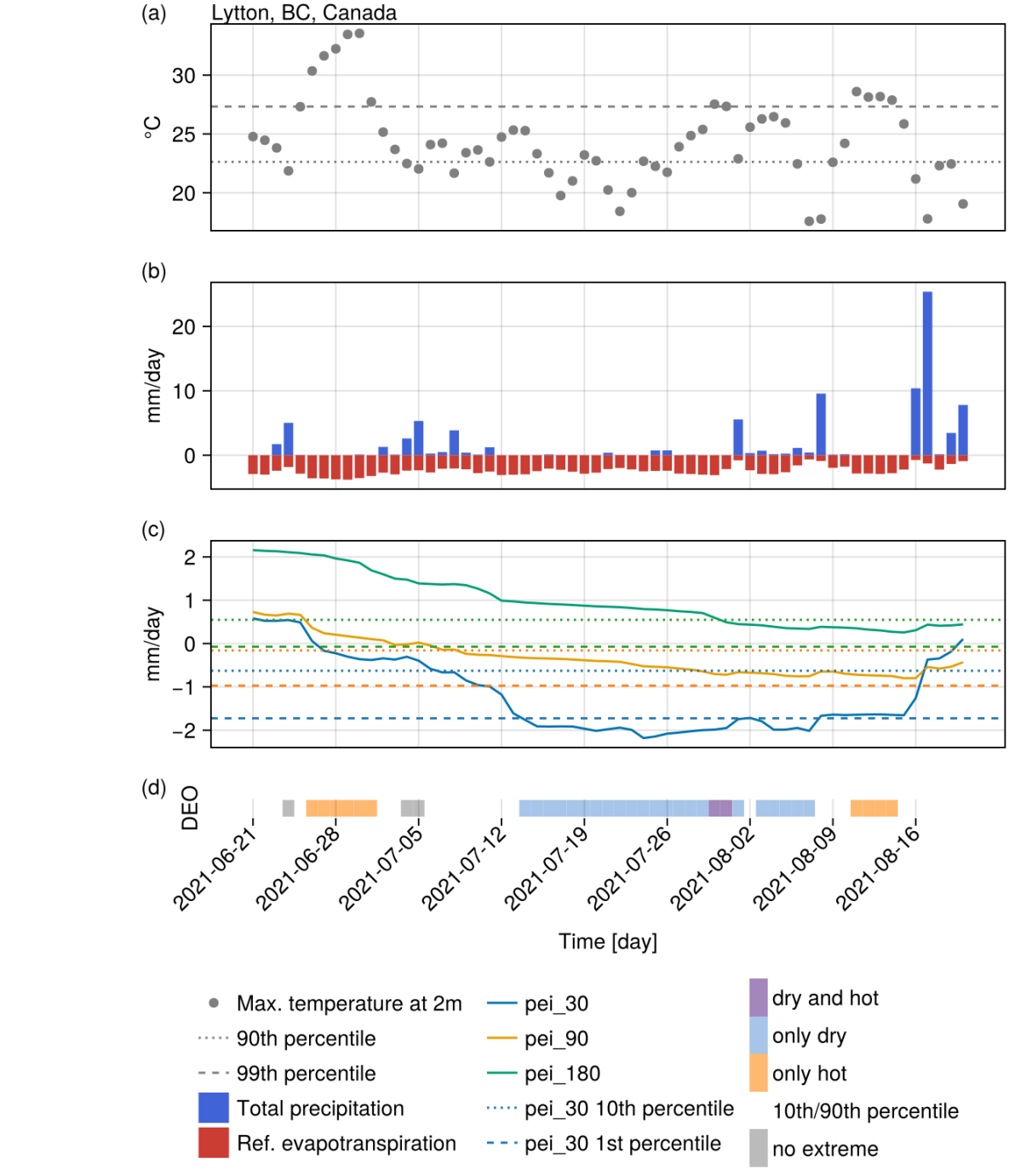

Figure 10. Reported compound dry and hot extreme event in British Colombia not associated with labelled event from the proposed database. Although dry and hot conditions were observed over its reported course, they did not coincide according to the stringent threshold used in this study. Panels show (a) the maximum daily temperature, (b) the daily precipitation and reference evapotranspiration, (c) the three drought indicators (PEI) and (d) the Discrete Extreme Occurrences (DEO).

https://doi.org/10.5194/essd-2024-396
Preprint. Discussion started: 18 October 2024

intensity. A combined cumulative metric for both dry and hot conditions would need particular attention. In their review, Hao et al. (2022) mention the Dry-Hot Magnitude Index (DHMI) of compound dry and hot extremes (Wu et al., 2019) valid for monthly input data. It could be adapted to deal with the daily data and with the multiple drought indicators used in Dheed.

5 Conclusions

In this data description paper, we propose Dheed, a daily dry and hot extreme events database based on ERA5 consisting of two data cubes and a table: (i) an EventCube of Discrete Extreme Occurrences (DEOs), i.e. days in which extremely dry and/or hot conditions were detected; (ii) a LabelCube of uniquely labelled Dry and Hot Extreme Events (DHEEs), i.e. blobs of simultaneously dry and hot DEOs connected in space and time; (iii) StatEvents, a table containing summary statistics for all labelled DHEEs. The analysis of the EventCube confirms that the occurrence of both dry and hot extremes as well as their co-occurrence has increased significantly in the past few decades. The trend is not homogeneous across all continents, with Europe and Africa seeing the strongest increase in the annual number of days and areas affected by DHEEs. The largest and longest DHEEs were tracked in the scientific literature and the Dheed was compared against a list of extreme events reported in the literature and collected a priori. The labelCube and its associated table allow the user to easily retrieve in time and space extremely dry and hot conditions, which have occurred, according to climate reanalysis data, between 1950 and 2022, to further study their impact on ecosystems and societies.

6 Code and data availability

Code associated with this study, including the full data processing to create the database of dry and hot extreme events, as well as the creation of the figures presented in this article, is available from zenodo/10.5281/zenodo.13711289 (Weynants et al., 2024a). The database of connected compound dry and hot extreme events is available from zenodo/10.5281/zenodo.11546130 (Weynants et al., 2024b). With no guarantee of permanent storage, all data cubes generated with the current workflow can currently be accessed on a public s3 bucket at https://s3.bgc-jena.mpg.de:9000/minio/deepextremes/v3/. A ReadMe file details the contents of the data store and how to access the data cubes with Julia or python: https://s3.bgc-jena.mpg.de:9000/minio/deepextremes/v3/ReadMe.md.

Appendix A: Supplementary material

A1 Time series from Dheed

Figure A1 shows the last five years of the timeseries for the four indicators ($T_{2m,max}$, PEI_{30}, PEI_{90}, and PEI_{180}) used in the detection of DEOs around the city of Jena, Germany (50.9° North, 11.59° West). Daily ET_{ref} and P are also shown in the background. At that particular location, the 1% threshold of maximum daily temperature obtained for the full timeseries (1950–2022) is 304.51 K, or 31.36 ° C. Such a threshold classifies as extremes only the summer hot days. The thresholds

https://doi.org/10.5194/essd-2024-396
Preprint. Discussion started: 18 October 2024

for the drought indicators are $PEI_{30} = -1.31$, $PEI_{90} = -0.82$ and $PEI_{180} = -0.43$ mm/day. 2018, 2019, 2020 and 2022 have been dry, with cumulative water deficit showing for all three PEI. At a location in a completely different climate zone, the thresholds will also be different. For example, around Niamey, Niger (13.5116° N, 2.1254° E, Fig A2), the thresholds are: $T_{2m,max} = 44.00$, $PEI_{30} = -5.02$, $PEI_{90} = -4.70$ and $PEI_{180} = -4.31$. In this Sahelian climate, a deficit in water is the norm rather than the exception.

https://doi.org/10.5194/essd-2024-396
Preprint. Discussion started: 18 October 2024

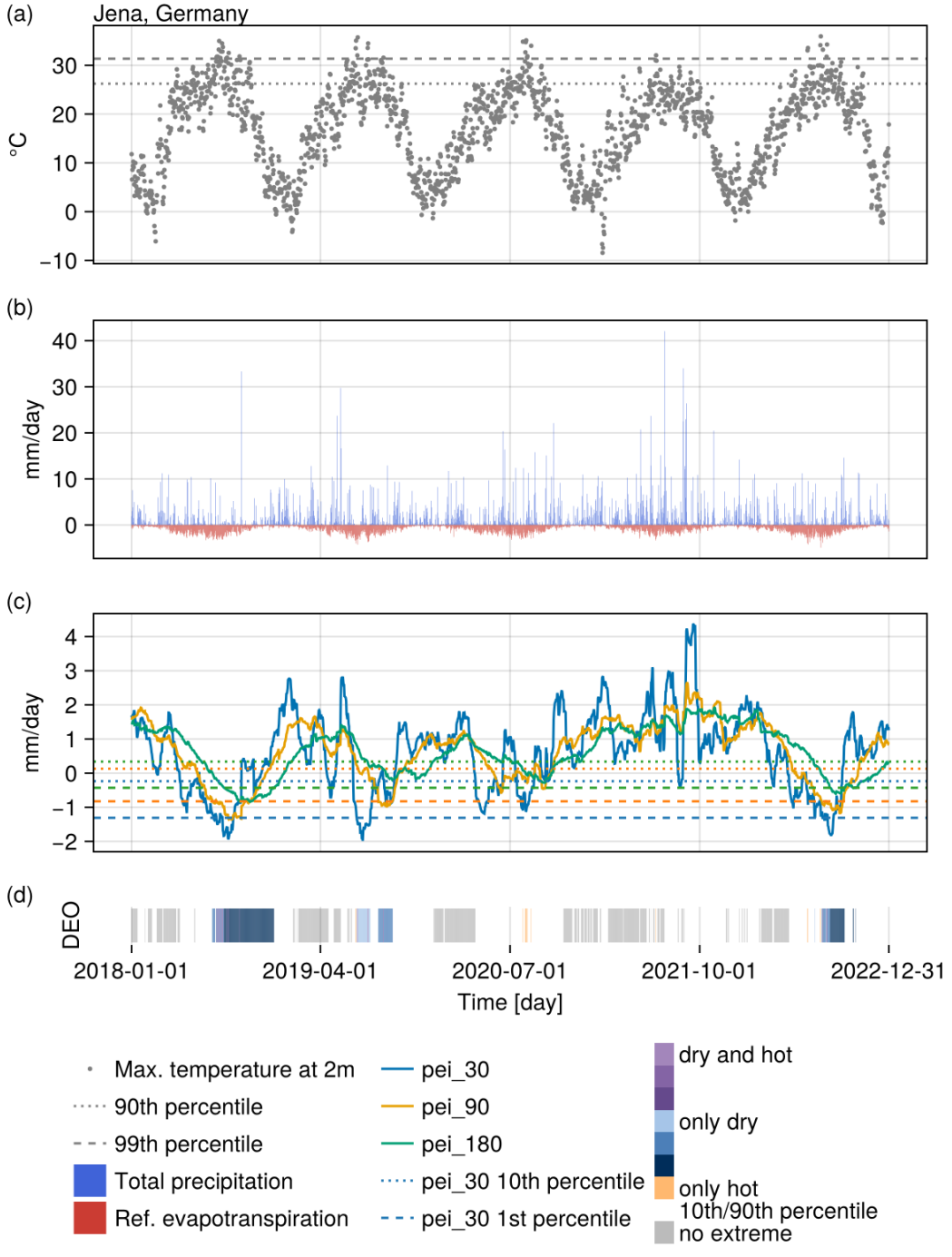

Figure A1. Timeseries (2018–2022) of (a) maximum daily temperature, (b) daily precipitation and reference evapotranspiration, (c) the three drought indicators (PEI) and (d) the Discrete Extreme Occurrences (DEO) around the city of Jena, Germany. The summers in those years (except 2021) were relatively dry, with very hot days resulting in compound dry and hot extremes in 2018, 2019 and 2022.

https://doi.org/10.5194/essd-2024-396
Preprint. Discussion started: 18 October 2024

Open Access Earth System Science Data Discussions

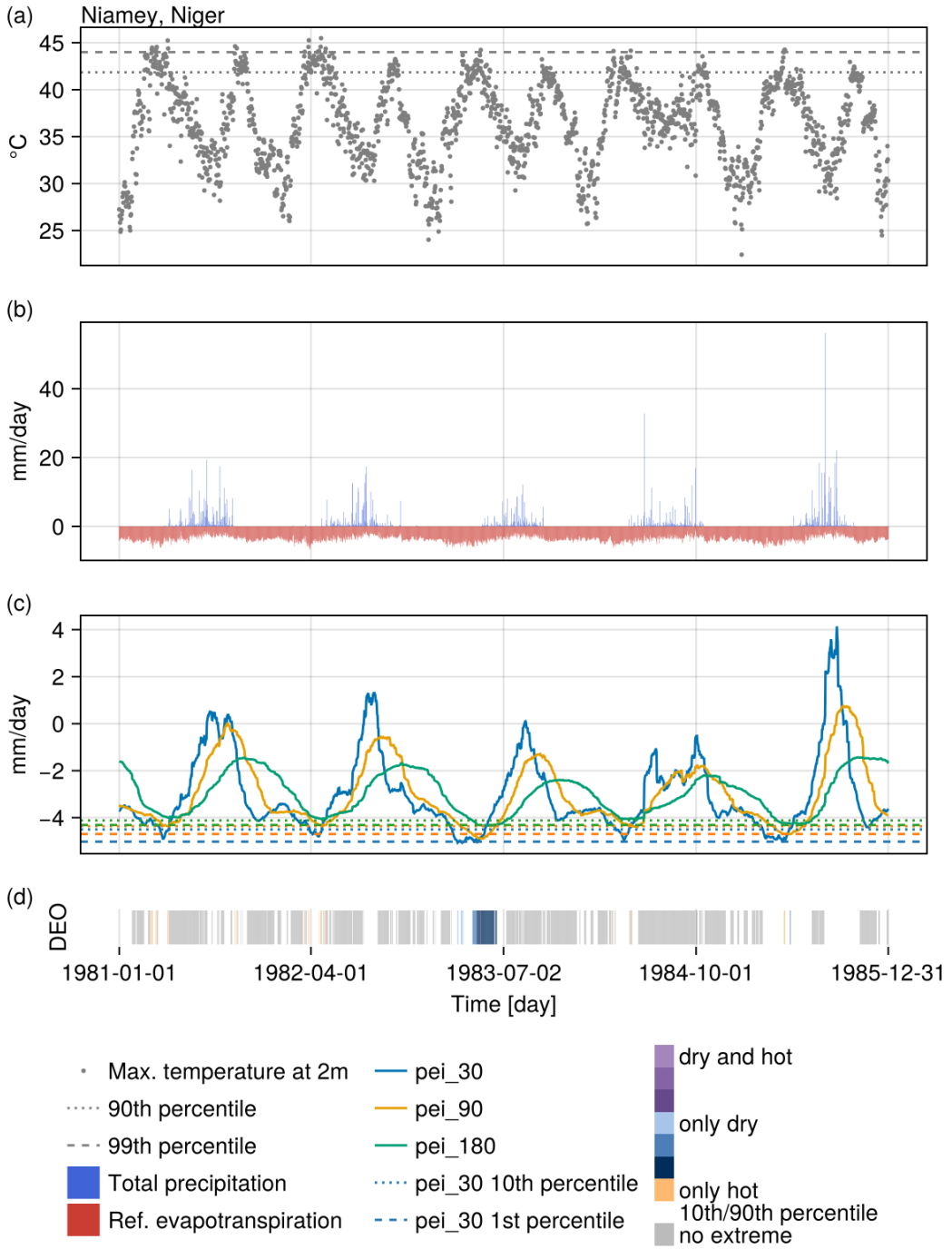

Figure A2. Timeseries (1981–1985) of (a) maximum daily temperature, (b) daily precipitation and reference evapotranspiration, (c) the three drought indicators (PEI) and (d) the Discrete Extreme Occurrences (DEO) around the city of Niamey, Niger. The year 1983 was very dry, but it had only one very hot day resulting in a compound dry and hot event that would not be labelled in Dheed, where events must last at least three days.

https://doi.org/10.5194/essd-2024-396
Preprint. Discussion started: 18 October 2024

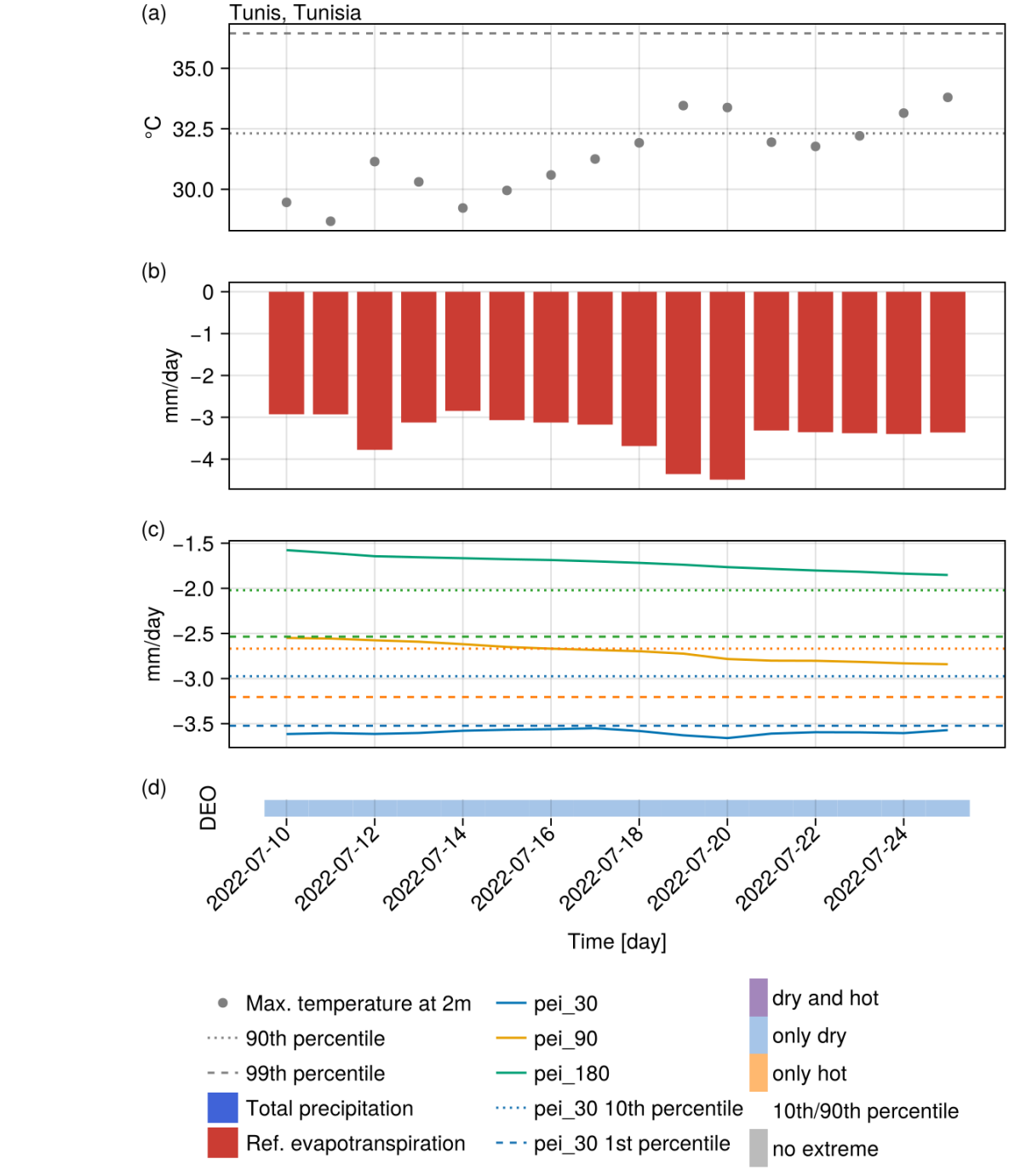

Figure A3. Reported compound dry and hot extreme event in Tunisia not associated with labelled event from the proposed database. Although dry conditions were observed over its reported course, the maximum temperature did not reach the stringent threshold used in this study. Panels show (a) the maximum daily temperature, (b) the daily precipitation and reference evapotranspiration, (c) the three drought indicators (PEI) and (d) the Discrete Extreme Occurrences (DEO).

https://doi.org/10.5194/essd-2024-396
Preprint. Discussion started: 18 October 2024

Open Access Earth System Science Data Discussions

A2 Supplementary table

https://doi.org/10.5194/essd-2024-396
Preprint. Discussion started: 18 October 2024

Open Access Earth System Science Data Discussions

Table A1. Extreme events reported in the literature or the media used to validate the event detection method.

Event	Region	Type	Start	End	West	East	South	North	Ref.
1	South Africa	heatwave	2016-01-01	2016-01-10	18.0	48.0	-35.0	-16.0	Meque et al. (2022)
2	South Africa	drought	2016-10-07	2017-01-30	18.0	48.0	-35.0	-16.0	Meque et al. (2022)
3	Pakistan	heatwave	2017-05-20	2017-06-02	60.5	77.25	23.5	37.25	Wikipedia (2017)
4	India-Pakistan	drought	2019-02-01	2019-06-30	61.0	89.0	7.0	34.0	Wikipedia (2019)
5	Europe	compound	2018-06-01	2018-08-31	-10.0	35.0	30.0	70.0	Liu et al. (2020)
6	Europe	compound	2019-06-01	2019-08-31	-10.0	35.0	30.0	70.0	Bastos et al. (2021)
7	Brazil	compound	2020-09-20	2020-11-10	-56.5	-18.5	-56.5	-18.5	Libonati et al. (2022)
8	Canada	compound	2021-06-20	2021-07-10	-127.0	-95.0	48.0	60.0	White et al. (2023)
9	Europe	drought	2022-03-01	2022-07-22	-10.0	37.0	30.0	54.0	Tripathy and Mishra (2023)
10	Europe	heatwave	2022-07-10	2022-7-22	-10.0	37.0	30.0	54.0	Tripathy and Mishra (2023)
11	India-Pakistan	compound	2022-03-15	2022-05-30	61.0	89.0	7.0	34.0	Aadhar and Mishra (2023)
12	India	heatwave	2016-04-01	2016-05-20	61.0	89.0	7.0	34.0	Singh et al. (2017)
13	India	heatwave	2017-04-12	2017-06-15	61.0	89.0	7.0	34.0	Hari and Tyagi (2021)
14	India	heatwave	2018-05-12	2018-06-10	61.0	89.0	7.0	34.0	Safi (2018); Hari and Tyagi (2021)
15	India	heatwave	2019-06-01	2019-06-30	61.0	89.0	7.0	34.0	Hari and Tyagi (2021)
16	India	heatwave	2022-03-01	2022-03-31	61.0	89.0	7.0	34.0	Aadhar and Mishra (2023)
17	USA	drought	2017-03-01	2017-12-31	-125.0	-70.0	25.0	50.0	NOAA (2018)
18	USA	drought	2020-01-01	2020-12-31	-125.0	-70.0	25.0	50.0	NOAA (2021)
19	USA	drought	2021-01-01	2021-12-31	-125.0	-70.0	25.0	50.0	NOAA (2022)
20	W. North America	heatwave	2021-06-25	2021-07-07	-140.0	-115.0	35.0	65.0	NOAA (2022)
21	Europe-middle	heatwave	2018-07-01	2018-07-30	-3.0	23.0	42.0	53.0	Rousi et al. (2023)
22	Europe-west	heatwave	2019-06-24	2019-06-30	-9.0	16.0	35.0	60.0	Xu et al. (2020)
23	Europe-midwest	heatwave	2020-06-01	2020-08-16	-9.0	5.0	42.0	60.0	Copernicus
24	Europe	heatwave	2022-07-10	2022-07-25	-10.0	35.0	30.0	70.0	Pratt (2022)
25	Tunisia	heatwave	2022-07-10	2022-07-25	7.5	12.0	30.0	38.0	Pratt (2022)
26	Iran	heatwave	2022-07-10	2022-07-25	44.0	63.5	24.5	40.03	Pratt (2022)
27	China	heatwave	2022-07-10	2022-07-25	53.5	73.5	8.5	135.0	Pratt (2022)
28	Texas, USA	compound	2011-06-01	2011-08-31	-106.65	-93.51	25.84	36.5	Nielsen-Gammon (2012)
29	Russia	heatwave	2010-06-01	2010-08-30	28.75	60.25	48.25	66.75	Flach et al. (2018)
30	Amazon	drought	2010-01-01	2010-12-31	-73.0	-64.0	-11.0	-4.0	Lewis et al. (2011)
31	USA*	drought	2005-11-01	2006-02-28	-100.0	-95.0	32.5	37.5	Dong et al. (2011)
32	Amazon	drought	2005-01-01	2005-12-31	-73.0	-64.0	-11.0	-4.0	Lewis et al. (2011)
33	Europe	drought	2003-07-01	2003-09-30	-10.0	35.0	35.0	65.0	Ciais et al. (2005)

continued on next page

https://doi.org/10.5194/essd-2024-396
Preprint. Discussion started: 18 October 2024

continued from previous page

obs_event	Region	Type	Start	End	West	East	South	North	Ref.
34	Europe	heatwave	2003-07-01	2003-08-31	-10.0	35.0	35.0	65.0	Ciais et al. (2005)
35	North Argentina	drought	1995-07-01	1996-06-30	-75.0	-56.0	-40.0	-24.0	Minetti et al. (2003)
36	North East Brazil	drought	1993-02-01	1993-05-31	-47.0	-35.0	-12.0	7.5	Rao et al. (1995)
37	Poland	drought	1992-09-01	1992-09-30	14.0	24.0	49.0	55.0	Łabędzki (2007)
38	USA	drought	1988-03-01	1988-07-31	-160.0	-50.0	30.0	60.0	Namias (1991)
39	Sahel	drought	1983-10-01	1984-09-30	-10.0	33.0	10.0	18.0	Tucker et al. (1986)

*Southern Great Plains

https://doi.org/10.5194/essd-2024-396
Preprint. Discussion started: 18 October 2024

Author contributions. MW, FG and NL in conversation with MDM and the Deep Extremes team designed the methodology. NL, FG and MW coded the workflow. UW retrieved and pre-processed the ERA5 data. CJ compiled the table of historic extreme events. MW ran the code, conducted the analyses and wrote the manuscript with contributions from all co-authors.

Competing interests. The authors declare that they have no conflict of interest.

Disclaimer. The data are provided as is, with no warranties.

Acknowledgements. This work was funded by the European Space Agency (ESA) AI4Science project "Multi-Hazards, Compounds and Cascade events: DeepExtremes," 2022–2024, and the European Union's Horizon 2020 research and innovation program within the project "XAIDA: Extreme Events – Artificial Intelligence for Detection and Attribution", (grant agreement 101003469). Recent developments in the Julia package YAXArrays.jl were funded by ESA AI4Science project "The DeepESDL AI-Ready Earth System Data Lab".

https://doi.org/10.5194/essd-2024-396
Preprint. Discussion started: 18 October 2024

References

ImageFiltering.jl, https://github.com/JuliaImages/ImageFiltering.jl, 2023a.

ImageMorphology.jl, https://github.com/JuliaImages/ImageMorphology.jl, 2023b.

Aadhar, S. and Mishra, V.: The 2022 mega heatwave in South Asia in the observed and projected future climate, Environmental Research Letters, 18, 104 011, https://doi.org/10.1088/1748-9326/acf778, publisher: IOP Publishing, 2023.

Allen, C. D., Macalady, A. K., Chenchouni, H., Bachelet, D., McDowell, N., Vennetier, M., Kitzberger, T., Rigling, A., Breshears, D. D., Hogg, E. T., Gonzalez, P., Fensham, R., Zhang, Z., Castro, J., Demidova, N., Lim, J.-H., Allard, G., Running, S. W., Semerci, A., and Cobb, N.: A global overview of drought and heat-induced tree mortality reveals emerging climate change risks for forests, Forest Ecology and Management, 259, 660–684, https://doi.org/10.1016/j.foreco.2009.09.001, 2010.

Allen, R. G., Pereira, L. S., Raes, D., and Smith, M.: Crop evapotranspiration - Guidelines for computing crop water requirements, FAO Irrigation and drainage, FAO - Food and Agriculture Organization of the United Nations, Rome, ISBN 92-5-104219-5, https://www.fao.org/3/x0490e/x0490e00.htm#Contents, 1998.

Bastos, A., Ciais, P., Friedlingstein, P., Sitch, S., Pongratz, J., Fan, L., Wigneron, J. P., Weber, U., Reichstein, M., Fu, Z., Anthoni, P., Arneth, A., Haverd, V., Jain, A. K., Joetzjer, E., Knauer, J., Lienert, S., Loughran, T., McGuire, P. C., Tian, H., Viovy, N., and Zaehle, S.: Direct and seasonal legacy effects of the 2018 heat wave and drought on European ecosystem productivity, Science Advances, 6, eaba2724, https://doi.org/10.1126/sciadv.aba2724, 2020.

Bastos, A., Orth, R., Reichstein, M., Ciais, P., Viovy, N., Zaehle, S., Anthoni, P., Arneth, A., Gentine, P., Joetzjer, E., Lienert, S., Loughran, T., McGuire, P. C., O, S., Pongratz, J., and Sitch, S.: Vulnerability of European ecosystems to two compound dry and hot summers in 2018 and 2019, Earth System Dynamics, 12, 1015–1035, https://doi.org/10.5194/esd-12-1015-2021, publisher: Copernicus GmbH, 2021.

Bastos, A., Sippel, S., Frank, D., Mahecha, M. D., Zaehle, S., Zscheischler, J., and Reichstein, M.: A joint framework for studying compound ecoclimatic events, Nature Reviews Earth & Environment, 4, 333–350, https://doi.org/10.1038/s43017-023-00410-3, 2023.

Benson, V., Robin, C., Requena-Mesa, C., Alonso, L., Carvalhais, N., Cortés, J., Gao, Z., Linscheid, N., Weynants, M., and Reichstein, M.: Multi-modal learning for geospatial vegetation forecasting, https://doi.org/10.48550/ARXIV.2303.16198, publisher: [object Object] Version Number: 2, 2023.

Cammalleri, C., Acosta Navarro, J. C., Bavera, D., Diaz, V., Di Ciollo, C., Maetens, W., Magni, D., Masante, D., Spinoni, J., and Toreti, A.: An event-oriented database of meteorological droughts in Europe based on spatio-temporal clustering, Scientific Reports, 13, 3145, https://doi.org/10.1038/s41598-023-30153-6, number: 1 Publisher: Nature Publishing Group, 2023.

Ciais, P., Reichstein, M., Viovy, N., Granier, A., Ogée, J., Allard, V., Aubinet, M., Buchmann, N., Bernhofer, C., Carrara, A., Chevallier, F., De Noblet, N., Friend, A. D., Friedlingstein, P., Grünwald, T., Heinesch, B., Keronen, P., Knohl, A., Krinner, G., Loustau, D., Manca, G., Matteucci, G., Miglietta, F., Ourcival, J. M., Papale, D., Pilegaard, K., Rambal, S., Seufert, G., Soussana, J. F., Sanz, M. J., Schulze, E. D., Vesala, T., and Valentini, R.: Europe-wide reduction in primary productivity caused by the heat and drought in 2003, Nature, 437, 529–533, https://doi.org/10.1038/nature03972, publisher: Nature Publishing Group, 2005.

Copernicus: Heatwaves and warm spells | Copernicus, https://climate.copernicus.eu/esotc/2020/heatwaves-and-warm-spells-during-2020.

Danisch, S. and Krumbiegel, J.: Makie.jl: Flexible high-performance data visualization for Julia, Journal of Open Source Software, 6, 3349, https://doi.org/10.21105/joss.03349, 2021.

Dong, X., Xi, B., Kennedy, A., Feng, Z., Entin, J. K., Houser, P. R., Schiffer, R. A., L'Ecuyer, T., Olson, W. S., Hsu, K.-l., Liu, W. T., Lin, B., Deng, Y., and Jiang, T.: Investigation of the 2006 drought and 2007 flood extremes at the Southern Great Plains through an

https://doi.org/10.5194/essd-2024-396
Preprint. Discussion started: 18 October 2024

integrative analysis of observations, Journal of Geophysical Research: Atmospheres, 116, https://doi.org/10.1029/2010JD014776, _eprint: https://onlinelibrary.wiley.com/doi/pdf/10.1029/2010JD014776, 2011.

Flach, M., Gans, F., Brenning, A., Denzler, J., Reichstein, M., Rodner, E., Bathiany, S., Bodesheim, P., Guanche, Y., Sippel, S., and Mahecha, M. D.: Multivariate anomaly detection for Earth observations: a comparison of algorithms and feature extraction techniques, Earth System Dynamics, 8, 677–696, https://doi.org/10.5194/esd-8-677-2017, 2017.

Flach, M., Sippel, S., Gans, F., Bastos, A., Brenning, A., Reichstein, M., and Mahecha, M. D.: Contrasting biosphere responses to hydrometeorological extremes: revisiting the 2010 western Russian heatwave, Biogeosciences, 15, 6067–6085, https://doi.org/10.5194/bg-15-6067-2018, 2018.

Flach, M., Brenning, A., Gans, F., Reichstein, M., Sippel, S., and Mahecha, M. D.: Vegetation modulates the impact of climate extremes on gross primary production, Biogeosciences, 18, 39–53, https://doi.org/10.5194/bg-18-39-2021, publisher: Copernicus GmbH, 2021.

Frank, D., Reichstein, M., Bahn, M., Thonicke, K., Frank, D., Mahecha, M. D., Smith, P., Van Der Velde, M., Vicca, S., Babst, F., Beer, C., Buchmann, N., Canadell, J. G., Ciais, P., Cramer, W., Ibrom, A., Miglietta, F., Poulter, B., Rammig, A., Seneviratne, S. I., Walz, A., Wattenbach, M., Zavala, M. A., and Zscheischler, J.: Effects of climate extremes on the terrestrial carbon cycle: concepts, processes and potential future impacts, Global Change Biology, 21, 2861–2880, https://doi.org/10.1111/gcb.12916, 2015.

Gans, F., Cremer, F., Alonso, L., Kraemer, G., Dimens, P. V., Gutwin, M., Pabon-Moreno, D. E., Kong, D., Martin, Martinuzzi, F., Chettouh, M. A., Loos, D., Zehner, M., Roy, P., Zhang, Q., ckrich, Glaser, F., and linamaes: JuliaDataCubes/YAXArrays.jl: v0.5.2, https://doi.org/10.5281/zenodo.8414000, 2023.

Hao, Z., Hao, F., Xia, Y., Feng, S., Sun, C., Zhang, X., Fu, Y., Hao, Y., Zhang, Y., and Meng, Y.: Compound droughts and hot extremes: Characteristics, drivers, changes, and impacts, Earth-Science Reviews, 235, 104 241, https://doi.org/10.1016/j.earscirev.2022.104241, 2022.

Hari, M. and Tyagi, B.: Investigating Indian summer heatwaves for 2017–2019 using reanalysis datasets, Acta Geophysica, 69, 1447–1464, https://doi.org/10.1007/s11600-021-00603-8, 2021.

Hassan, M., Saif, K., Ijaz, M. S., Sarfraz, Z., Sarfraz, A., Robles-Velasco, K., and Cherrez-Ojeda, I.: Mean Temperature and Drought Projections in Central Africa: A Population-Based Study of Food Insecurity, Childhood Malnutrition and Mortality, and Infectious Disease, International Journal of Environmental Research and Public Health, 20, 2697, https://doi.org/10.3390/ijerph20032697, 2023.

Hersbach, H.: ERA5 reanalysis now available from 1940, https://www.ecmwf.int/en/newsletter/175/news/era5-reanalysis-now-available-1940, 2023.

Hersbach, H., Bell, B., Berrisford, P., Hirahara, S., Horányi, A., Muñoz-Sabater, J., Nicolas, J., Peubey, C., Radu, R., Schepers, D., Simmons, A., Soci, C., Abdalla, S., Abellan, X., Balsamo, G., Bechtold, P., Biavati, G., Bidlot, J., Bonavita, M., Chiara, G., Dahlgren, P., Dee, D., Diamantakis, M., Dragani, R., Flemming, J., Forbes, R., Fuentes, M., Geer, A., Haimberger, L., Healy, S., Hogan, R. J., Hólm, E., Janisková, M., Keeley, S., Laloyaux, P., Lopez, P., Lupu, C., Radnoti, G., Rosnay, P., Rozum, I., Vamborg, F., Villaume, S., and Thépaut, J.: The ERA5 global reanalysis, Quarterly Journal of the Royal Meteorological Society, 146, 1999–2049, https://doi.org/10.1002/qj.3803, 2020.

Hersbach, H., Bell, B., Berrisford, P., Biavati, G., Horányi, A., Muñoz-Sabater, J., Nicolas, J., Peubey, C., Radu, R., Rozum, I., Schepers, D., Simmons, A., Soci, C., Dee, D., and Thépaut, J.: ERA5 hourly data on single levels from 1940 to present, https://doi.org/10.24381/cds.adbb2d47, 2023.

IPCC: Managing the Risks of Extreme Events and Disasters to Advance Climate Change Adaptation - A Special Report of Working Groups I and II of the Intergovernmental Panel on Climate Change, Cambridge University Press, https://www.ipcc.ch/report/managing-the-risks-of-extreme-events-and-disasters-to-advance-climate-change-adaptation/, 2012.

https://doi.org/10.5194/essd-2024-396
Preprint. Discussion started: 18 October 2024

Ji, C., Fincke, T., Benson, V., Camps-Valls, G., Fernandez-Torres, M.-A., Gans, F., Kraemer, G., Martinuzzi, F., Montero, D., Mora, K., Pellicer-Valero, O. J., Robin, C., Soechting, M., Weynants, M., and Mahecha, M. D.: DeepExtremeCubes: Integrating Earth system spatio-temporal data for impact assessment of climate extremes, https://arxiv.org/abs/2406.18179, 2024.

Lavaysse, C., Cammalleri, C., Dosio, A., van der Schrier, G., Toreti, A., and Vogt, J.: Towards a monitoring system of temperature extremes in Europe, Natural Hazards and Earth System Sciences, 18, 91–104, https://doi.org/10.5194/nhess-18-91-2018, publisher: Copernicus GmbH, 2018.

Lewis, S. L., Brando, P. M., Phillips, O. L., van der Heijden, G. M. F., and Nepstad, D.: The 2010 Amazon Drought, Science, 331, 554–554, https://doi.org/10.1126/science.1200807, publisher: American Association for the Advancement of Science, 2011.

Li, J., Wang, Z., Wu, X., Zscheischler, J., Guo, S., and Chen, X.: A standardized index for assessing sub-monthly compound dry and hot conditions with application in China, Hydrology and Earth System Sciences, 25, 1587–1601, https://doi.org/10.5194/hess-25-1587-2021, 2021.

Libonati, R., Geirinhas, J. L., Silva, P. S., Russo, A., Rodrigues, J. A., Belém, L. B. C., Nogueira, J., Roque, F. O., DaCamara, C. C., Nunes, A. M. B., Marengo, J. A., and Trigo, R. M.: Assessing the role of compound drought and heatwave events on unprecedented 2020 wildfires in the Pantanal, Environmental Research Letters, 17, 015 005, https://doi.org/10.1088/1748-9326/ac462e, publisher: IOP Publishing, 2022.

Liu, X., He, B., Guo, L., Huang, L., and Chen, D.: Similarities and Differences in the Mechanisms Causing the European Summer Heatwaves in 2003, 2010, and 2018, Earth's Future, 8, e2019EF001 386, https://doi.org/10.1029/2019EF001386, _eprint: https://onlinelibrary.wiley.com/doi/pdf/10.1029/2019EF001386, 2020.

Lloyd-Hughes, B.: A spatio-temporal structure-based approach to drought characterisation, International Journal of Climatology, 32, 406–418, https://doi.org/10.1002/joc.2280, _eprint: https://onlinelibrary.wiley.com/doi/pdf/10.1002/joc.2280, 2012.

Mahecha, M. D., Gans, F., Sippel, S., Donges, J. F., Kaminski, T., Metzger, S., Migliavacca, M., Papale, D., Rammig, A., and Zscheischler, J.: Detecting impacts of extreme events with ecological in situ monitoring networks, Biogeosciences, 14, 4255–4277, https://doi.org/10.5194/bg-14-4255-2017, 2017.

Mahecha, M. D., Gans, F., Brandt, G., Christiansen, R., Cornell, S. E., Fomferra, N., Kraemer, G., Peters, J., Bodesheim, P., Camps-Valls, G., Donges, J. F., Dorigo, W., Estupinan-Suarez, L. M., Gutierrez-Velez, V. H., Gutwin, M., Jung, M., Londoño, M. C., Miralles, D. G., Papastefanou, P., and Reichstein, M.: Earth system data cubes unravel global multivariate dynamics, Earth System Dynamics, 11, 201–234, https://doi.org/10.5194/esd-11-201-2020, publisher: Copernicus GmbH, 2020.

Mahecha, M. D., Bastos, A., Bohn, F. J., Eisenhauer, N., Feilhauer, H., Hickler, T., Kalesse-Los, H., Migliavacca, M., Otto, F. E. L., Peng, J., Sippel, S., Tegen, I., Weigelt, A., Wendisch, M., Wirth, C., Al-Halbouni, D., Deneke, H., Doktor, D., Dunker, S., Duveiller, G., Ehrlich, A., Foth, A., García-García, A., Guerra, C. A., Guimarães-Steinicke, C., Hartmann, H., Henning, S., Herrmann, H., Hu, P., Ji, C., Kattenborn, T., Kolleck, N., Kretschmer, M., Kühn, I., Luttkus, M. L., Maahn, M., Mönks, M., Mora, K., Pöhlker, M., Reichstein, M., Rüger, N., Sánchez-Parra, B., Schäfer, M., Stratmann, F., Tesche, M., Wehner, B., Wieneke, S., Winkler, A. J., Wolf, S., Zaehle, S., Zscheischler, J., and Quaas, J.: Biodiversity and Climate Extremes: Known Interactions and Research Gaps, Earth's Future, 12, e2023EF003 963, https://doi.org/10.1029/2023EF003963, 2024.

Marchin, R. M., Backes, D., Ossola, A., Leishman, M. R., Tjoelker, M. G., and Ellsworth, D. S.: Extreme heat increases stomatal conductance and drought-induced mortality risk in vulnerable plant species, Global Change Biology, 28, 1133–1146, https://doi.org/10.1111/gcb.15976, _eprint: https://onlinelibrary.wiley.com/doi/pdf/10.1111/gcb.15976, 2022.

https://doi.org/10.5194/essd-2024-396
Preprint. Discussion started: 18 October 2024

Marengo, J. A., Ambrizzi, T., Barreto, N., Cunha, A. P., Ramos, A. M., Skansi, M., Molina Carpio, J., and Salinas, R.: The heat wave of October 2020 in central South America, International Journal of Climatology, 42, 2281–2298, https://doi.org/10.1002/joc.7365, _eprint: https://onlinelibrary.wiley.com/doi/pdf/10.1002/joc.7365, 2022.

Masih, I., Maskey, S., Mussá, F. E. F., and Trambauer, P.: A review of droughts on the African continent: a geospatial and long-term perspective, Hydrology and Earth System Sciences, 18, 3635–3649, https://doi.org/10.5194/hess-18-3635-2014, 2014.

McDowell, N. G., Sapes, G., Pivovaroff, A., Adams, H. D., Allen, C. D., Anderegg, W. R. L., Arend, M., Breshears, D. D., Brodribb, T., Choat, B., Cochard, H., De Cáceres, M., De Kauwe, M. G., Grossiord, C., Hammond, W. M., Hartmann, H., Hoch, G., Kahmen, A., Klein, T., Mackay, D. S., Mantova, M., Martínez-Vilalta, J., Medlyn, B. E., Mencuccini, M., Nardini, A., Oliveira, R. S., Sala, A., Tissue, D. T., Torres-Ruiz, J. M., Trowbridge, A. M., Trugman, A. T., Wiley, E., and Xu, C.: Mechanisms of woody-plant mortality under rising drought, CO2 and vapour pressure deficit, Nature Reviews Earth & Environment, 3, 294–308, https://doi.org/10.1038/s43017-022-00272-1, publisher: Nature Publishing Group, 2022.

Meque, A., Pinto, I., Maúre, G., and Beleza, A.: Understanding the variability of heatwave characteristics in southern Africa, Weather and Climate Extremes, 38, https://doi.org/10.1016/j.wace.2022.100498, 2022.

Minetti, J. L., Vargas, W. M., Poblete, A. G., Acuña, L. R., and Casagrande, G.: Non-linear trends and low frequency oscillations in annual precipitation over Argentina and Chile, 1931-1999, Atmósfera, 16, 119–135, http://www.scielo.org.mx/scielo.php?script=sci_abstract&pid=S0187-62362003000200004&lng=es&nrm=iso&tlng=en, publisher: Centro de Ciencias de la Atmósfera, UNAM, 2003.

Mishra, A. K. and Singh, V. P.: A review of drought concepts, Journal of Hydrology, 391, 202–216, https://doi.org/10.1016/j.jhydrol.2010.07.012, 2010.

Namias, J.: Spring and Summer 1988 Drought over the Contiguous United States–Causes and Prediction., Journal of Climate, 4, 54–65, https://doi.org/10.1175/1520-0442(1991)004<0054:SASDOT>2.0.CO;2, aDS Bibcode: 1991JCli....4...54N, 1991.

Nielsen-Gammon, J. W.: The 2011 Texas Drought, Texas Water Journal, 3, 59–95, https://doi.org/10.21423/twj.v3i1.6463, number: 1, 2012.

Niggli, L., Huggel, C., Muccione, V., Neukom, R., and Salzmann, N.: Towards improved understanding of cascading and interconnected risks from concurrent weather extremes: Analysis of historical heat and drought extreme events, PLOS Climate, 1, e0000057, https://doi.org/10.1371/journal.pclm.0000057, 2022.

NOAA: Annual 2017 Drought Report, https://www.ncei.noaa.gov/access/monitoring/monthly-report/drought/201713, 2018.

NOAA: Annual 2020 Drought Report, https://www.ncei.noaa.gov/access/monitoring/monthly-report/drought/202013, 2021.

NOAA: Annual 2021 Drought Report, https://www.ncei.noaa.gov/access/monitoring/monthly-report/drought/202113, 2022.

Perkins, S. E. and Alexander, L. V.: On the Measurement of Heat Waves, Journal of Climate, 26, 4500–4517, https://doi.org/10.1175/JCLI-D-12-00383.1, publisher: American Meteorological Society Section: Journal of Climate, 2013.

Pohl, F., Rakovec, O., Rebmann, C., Hildebrandt, A., Boeing, F., Hermanns, F., Attinger, S., Samaniego, L., and Kumar, R.: Long-term daily hydrometeorological drought indices, soil moisture, and evapotranspiration for ICOS sites, preprint, In Review, https://doi.org/10.21203/rs.3.rs-2516603/v1, 2023.

Pratt, S. E.: Heatwaves and Fires Scorch Europe, Africa, and Asia, https://earthobservatory.nasa.gov/images/150083/heatwaves-and-firesscorch-europe-africa-and-asia, publisher: NASA Earth Observatory, 2022.

Rao, V. B., Hada, K., and Herdies, D. L.: On the severe drought of 1993 in north-east Brazil, International Journal of Climatology, 15, 697–704, https://doi.org/10.1002/joc.3370150608, _eprint: https://onlinelibrary.wiley.com/doi/pdf/10.1002/joc.3370150608, 1995.

https://doi.org/10.5194/essd-2024-396
Preprint. Discussion started: 18 October 2024

Requena-Mesa, C., Benson, V., Reichstein, M., Runge, J., and Denzler, J.: EarthNet2021: A large-scale dataset and challenge for Earth surface forecasting as a guided video prediction task., in: Proceedings of the IEEE/CVF Conference on Computer Vision and Pattern Recognition, pp. 1132–1142, 2021.

Rippey, B. R.: The U.S. drought of 2012, Weather and Climate Extremes, 10, 57–64, https://doi.org/10.1016/j.wace.2015.10.004, 2015.

Rodell, M. and Li, B.: Changing intensity of hydroclimatic extreme events revealed by GRACE and GRACE-FO, Nature Water, 1, 241–248, https://doi.org/10.1038/s44221-023-00040-5, number: 3 Publisher: Nature Publishing Group, 2023.

Rouault, M., Dieppois, B., Tim, N., Hünicke, B., and Zorita, E.: Southern Africa Climate Over the Recent Decades: Description, Variability and Trends, in: Sustainability of Southern African Ecosystems under Global Change: Science for Management and Policy Interventions, edited by von Maltitz, G. P., Midgley, G. F., Veitch, J., Brümmer, C., Rötter, R. P., Viehberg, F. A., and Veste, M., pp. 149–168, Springer International Publishing, Cham, ISBN 978-3-031-10948-5, https://doi.org/10.1007/978-3-031-10948-5_6, 2024.

Rousi, E., Fink, A. H., Andersen, L. S., Becker, F. N., Beobide-Arsuaga, G., Breil, M., Cozzi, G., Heinke, J., Jach, L., Niermann, D., Petrovic, D., Richling, A., Riebold, J., Steidl, S., Suarez-Gutierrez, L., Tradowsky, J. S., Coumou, D., Düsterhus, A., Ellsäßer, F., Fragkoulidis, G., Gliksman, D., Handorf, D., Haustein, K., Kornhuber, K., Kunstmann, H., Pinto, J. G., Warrach-Sagi, K., and Xoplaki, E.: The extremely hot and dry 2018 summer in central and northern Europe from a multi-faceted weather and climate perspective, Natural Hazards and Earth System Sciences, 23, 1699–1718, https://doi.org/10.5194/nhess-23-1699-2023, publisher: Copernicus GmbH, 2023.

Russo, E. and Domeisen, D. I. V.: Increasing Intensity of Extreme Heatwaves: The Crucial Role of Metrics, Geophysical Research Letters, 50, e2023GL103 540, https://doi.org/10.1029/2023GL103540, _eprint: https://onlinelibrary.wiley.com/doi/pdf/10.1029/2023GL103540, 2023.

Russo, S., Sillmann, J., and Fischer, E. M.: Top ten European heatwaves since 1950 and their occurrence in the coming decades, Environmental Research Letters, 10, 124 003, https://doi.org/10.1088/1748-9326/10/12/124003, publisher: IOP Publishing, 2015.

Safi, M.: India slashes heatwave death toll with series of low-cost measures, https://www.theguardian.com/world/2018/jun/02/india-heat-wave-deaths-public-health-measures, publisher: The Guardian, 2018.

Seneviratne, S., Zhang, X., Adnan, M., Badi, W., Dereczynski, C., A. Di Luca, S. Ghosh, I. Iskandar, J. Kossin, F. Otto, I. Pinto, M. Satoh, S.M. Vicente-Serrano, M. Wehner, and B. Zhou: 2021: Weather and Climate Extreme Events in a Changing Climate, in: Climate Change 2021 – The Physical Science Basis: Working Group I Contribution to the Sixth Assessment Report of the Intergovernmental Panel on Climate Change, Cambridge University Press, 1 edn., ISBN 978-1-00-915789-6, https://doi.org/10.1017/9781009157896.013, 2023.

Singer, M. B., Asfaw, D. T., Rosolem, R., Cuthbert, M. O., Miralles, D. G., MacLeod, D., Quichimbo, E. A., and Michaelides, K.: Hourly potential evapotranspiration at 0.1° resolution for the global land surface from 1981-present, Scientific Data, 8, 224, https://doi.org/10.1038/s41597-021-01003-9, publisher: Nature Publishing Group, 2021.

Singh, H., Arora, K., Ashrit, R., and Rajagopal, E. N.: Verification of pre-monsoon temperature forecasts over India during 2016 with a focus on heatwave prediction, Natural Hazards and Earth System Sciences, 17, 1469–1485, https://doi.org/10.5194/nhess-17-1469-2017, publisher: Copernicus GmbH, 2017.

Sippel, S., Reichstein, M., Ma, X., Mahecha, M. D., Lange, H., Flach, M., and Frank, D.: Drought, Heat, and the Carbon Cycle: a Review, Current Climate Change Reports, 4, 266–286, https://doi.org/10.1007/s40641-018-0103-4, 2018.

Tripathy, K. P. and Mishra, A. K.: How Unusual Is the 2022 European Compound Drought and Heatwave Event?, Geophysical Research Letters, 50, e2023GL105 453, https://doi.org/10.1029/2023GL105453, _eprint: https://onlinelibrary.wiley.com/doi/pdf/10.1029/2023GL105453, 2023.

https://doi.org/10.5194/essd-2024-396
Preprint. Discussion started: 18 October 2024

Tucker, C. J., Justice, C. O., and Prince, S. D.: Monitoring the grasslands of the Sahel 1984-1985, International Journal of Remote Sensing, 7, 1571–1581, https://doi.org/10.1080/01431168608948954, publisher: Taylor & Francis _eprint: https://doi.org/10.1080/01431168608948954, 1986.

Vicente-Serrano, S. M., Beguería, S., and López-Moreno, J. I.: A Multiscalar Drought Index Sensitive to Global Warming: The Standardized Precipitation Evapotranspiration Index, Journal of Climate, 23, 1696–1718, https://doi.org/10.1175/2009JCLI2909.1, 2010.

Walter, I. A., Allen, R. G., Elliott, R., Jensen, M. E., Itenfisu, D., Mecham, B., Howell, T. A., Snyder, R., Brown, P., Echings, S., Spofford, T., Hattendorf, M., Cuenca, R. H., Wright, J. L., and Martin, D.: ASCE's Standardized Reference Evapotranspiration Equation, in: Watershed Management and Operations Management 2000, pp. 1–11, American Society of Civil Engineers, Fort Collins, Colorado, United States, ISBN 978-0-7844-0499-7, https://doi.org/10.1061/40499(2000)126, 2001.

Wang, Q., Zeng, J., Qi, J., Zhang, X., Zeng, Y., Shui, W., Xu, Z., Zhang, R., Wu, X., and Cong, J.: A multi-scale daily SPEI dataset for drought characterization at observation stations over mainland China from 1961 to 2018, Earth System Science Data, 13, 331–341, https://doi.org/10.5194/essd-13-331-2021, 2021.

Weng, W., Becker, S. L., Lüdeke, M. K. B., and Lakes, T.: Landscape matters: Insights from the impact of mega-droughts on Colombia's energy transition, Environmental Innovation and Societal Transitions, 36, 1–16, https://doi.org/10.1016/j.eist.2020.04.003, 2020.

Weynants, M., Linscheid, N., and Gans, F.: DeepExtremes/ExtremeEvents: v3.0.0, https://doi.org/10.5281/zenodo.13711289, 2024a.

Weynants, M., Linscheid, N., and Gans, F.: Dheed : a global database of dry and hot extreme events v3.0, https://doi.org/10.5281/zenodo.11546130, 2024b.

White, R. H., Anderson, S., Booth, J. F., Braich, G., Draeger, C., Fei, C., Harley, C. D. G., Henderson, S. B., Jakob, M., Lau, C.-A., Mareshet Admasu, L., Narinesingh, V., Rodell, C., Roocroft, E., Weinberger, K. R., and West, G.: The unprecedented Pacific Northwest heatwave of June 2021, Nature Communications, 14, 727, https://doi.org/10.1038/s41467-023-36289-3, publisher: Nature Publishing Group, 2023.

Wikipedia: https://en.wikipedia.org/wiki/2017_Pakistan_heat_wave, 2017.

Wikipedia: https://en.wikipedia.org/wiki/2019_heat_wave_in_India_and_Pakistan, 2019.

Wu, X., Hao, Z., Hao, F., Singh, V. P., and Zhang, X.: Dry-hot magnitude index: a joint indicator for compound event analysis, Environmental Research Letters, 14, 064 017, https://doi.org/10.1088/1748-9326/ab1ec7, publisher: IOP Publishing, 2019.

Xu, P., Wang, L., Liu, Y., Chen, W., and Huang, P.: The record-breaking heat wave of June 2019 in Central Europe, Atmospheric Science Letters, 21, e964, https://doi.org/10.1002/asl.964, _eprint: https://onlinelibrary.wiley.com/doi/pdf/10.1002/asl.964, 2020.

Yang, H., Munson, S. M., Huntingford, C., Carvalhais, N., Knapp, A. K., Li, X., Peñuelas, J., Zscheischler, J., and Chen, A.: The detection and attribution of extreme reductions in vegetation growth across the global land surface, Global Change Biology, 29, 2351–2362, https://doi.org/10.1111/gcb.16595, 2023.

Zscheischler, J., Mahecha, M. D., Harmeling, S., and Reichstein, M.: Detection and attribution of large spatiotemporal extreme events in Earth observation data, Ecological Informatics, 15, 66–73, https://doi.org/10.1016/j.ecoinf.2013.03.004, 2013.

Zscheischler, J., Martius, O., Westra, S., Bevacqua, E., Raymond, C., Horton, R. M., Van Den Hurk, B., AghaKouchak, A., Jézéquel, A., Mahecha, M. D., Maraun, D., Ramos, A. M., Ridder, N. N., Thiery, W., and Vignotto, E.: A typology of compound weather and climate events, Nature Reviews Earth & Environment, 1, 333–347, https://doi.org/10.1038/s43017-020-0060-z, 2020.

Łabędzki, L.: Estimation of local drought frequency in central Poland using the standardized precipitation index SPI, Irrigation and Drainage, 56, 67–77, https://doi.org/10.1002/ird.285, _eprint: https://onlinelibrary.wiley.com/doi/pdf/10.1002/ird.285, 2007.